Review

A Critical Review of Polymer Electrolyte Membrane Fuel Cell Systems for Automotive Applications: Components, Materials, and Comparative Assessment

Rolando Pedicini [1,*] **, Marcello Romagnoli** [2,3] **and Paolo E. Santangelo** [3,4]

1   CNR ITAE—Istituto di Tecnologie Avanzate per l'Energia "Nicola Giordano", 98126 Messina, Italy
2   Dipartimento di Ingegneria "Enzo Ferrari", Università degli Studi di Modena e Reggio Emilia,
    41125 Modena, Italy; marcello.romagnoli@unimore.it
3   Centro Interdipartimentale di Ricerca e per i Servizi nel settore della produzione, stoccaggio e utilizzo
    dell'Idrogeno H2—MO.RE., 41121 Modena, Italy; paoloemilio.santangelo@unimore.it
4   Dipartimento di Scienze e Metodi dell'Ingegneria, Università degli Studi di Modena e Reggio Emilia,
    42122 Reggio Emilia, Italy
*   Correspondence: rolando.pedicini@itae.cnr.it; Tel.: +39-090-624-277

Abstract: The development of innovative technologies based on employing green energy carriers, such as hydrogen, is becoming high in demand, especially in the automotive sector, as a result of the challenges associated with sustainable mobility. In the present review, a detailed overview of the entire hydrogen supply chain is proposed, spanning from its production to storage and final use in cars. Notably, the main focus is on Polymer Electrolyte Membrane Fuel Cells (PEMFC) as the fuel-cell type most typically used in fuel cell electric vehicles. The analysis also includes a cost assessment of the various systems involved; specifically, the materials commonly employed to manufacture fuel cells, stacks, and hydrogen storage systems are considered, emphasizing the strengths and weaknesses of the selected strategies, together with assessing the solutions to current problems. Moreover, as a sought-after parallelism, a comparison is also proposed and discussed between traditional diesel or gasoline cars, battery-powered electric cars, and fuel cell electric cars, thus highlighting the advantages and main drawbacks of the propulsion systems currently available on the market.

Keywords: Polymer Electrolyte Membrane Fuel Cell system; hydrogen production; hydrogen storage; hydrogen supply chain; fuel cell vehicles; electric vehicles; internal combustion engines; comparative analysis; cost assessment

1. Introduction

One of the main scopes of human society is to increase the possibility for everyone to move quickly, over both long and short distances. In all the past epochs of human history, traveling capability was limited by the means of transport then available, when carrying people, goods, or both. Human-powered (e.g., on foot), animal-powered (e.g., horses), and wind-powered (e.g., sailboats) modes of transport were the only ones available to our ancestors. When traveling on the ground, that limited the maximum distance covered in a daily journey down to a few tens of kilometers. Moreover, relatively few people were sufficiently wealthy to afford long trips, which also emphasizes the need for making means of transport economically viable to as many people as possible. More recently, the availability of abundant energy at a low price, such as oil, together with the dramatic rise of technological development and the industrial economy has made it possible to put efficient means of transport in the market, with prices that are affordable to a substantial share of the population. That has allowed the development of the current—and arguably complex—transport network and infrastructure, which is composed of the following sectors:

automotive, railway, naval, and air [1–7]. All of them feature some kind of propulsion system or power supply. After the first steam vehicle in 1769, exhibiting an exceptional maximum speed of 3.2 km/h, arguably unmatched at the time, the first car featuring an internal combustion engine was constructed in 1803. Quite remarkably, hydrogen was used as the fuel. Electric cars also appeared in the late 1800s, but they proved impractical, as a result of the poor performance in terms of the power available at the wheels [1]. The world had to wait until the second half of the XIX century to see the first cars propelled by fossil fuels [2]. In the twentieth century, the expansion of engines that run on fossil fuels was dramatic: petrol and diesel were first, followed by methane and LPG (liquified petroleum gas). However, the beginning of the twenty-first century seems to favor the return of electric cars, the most common types of which are BEVs (battery electric vehicles) [6] and FCEVs (fuel cell electric vehicles) or FCHEVs (fuel cell hybrid electric vehicles), with the last ones featuring both a fuel-cell stack and a battery pack [7].

From a physical standpoint, the engine has the function of overcoming the different forces that oppose motion: not only shall it ultimately provide kinetic energy to the whole mass of the car and the enclosed bodies, but it shall also balance against resistance. This latter typically includes tire-rolling resistance, aerodynamic drag, and uphill resistance [3–5]. As a well-known operating principle, an ICE (internal combustion engine) is propelled by the combustion of an air/fuel mixture within the cylinder. Such a combustion reaction has heat and gas as its products, with the latter expanding and forcing the piston to move down along the cylinder axis. The connection rod converts the translational motion of the piston into the rotational motion of the crankshaft, thus ultimately resulting in roto-translation of the wheels. The overall efficiency of ICE is known as not being particularly high. For instance, if the Otto—Beau de Rochas cycle is considered the ideal cycle for modeling spark-ignition engines fueled by gasoline [8], the following equation describes its thermal efficiency η:

$$\eta = 1 - \frac{1}{r_v^{\gamma-1}}, \tag{1}$$

where r_v is the compression ratio (i.e., the ratio between the volume of the cylinder with the piston at the bottom position and the same volume with the piston at the top position) and γ is the air heat capacity ratio. The latter is about 1.4 (i.e., that of a mixture of diatomic gases), so an increase in r_v yields an increase in η. However, the compression ratio may not be infinitely increased; for spark-ignition engines, if the compression ratio grows above about 10.5, a detonation phenomenon known as knocking occurs. This is detrimental to engine performance and, if persistent, may result in damage to the engine. Therefore, thermal efficiency of gasoline-fueled engines is limited by inherent maximum applicable values of the compression ratio; the same limitation holds for diesel (i.e., self-ignition) engines, yet their maximum compression ratio is higher. The overall efficiency of an ICE with a compression ratio of 8 is about 30%, generally ranging from 30% to 35%. Many factors contribute to make it even lower than thermal efficiency (i.e., a maximum possible threshold), among which non-instantaneous burning, incomplete combustion of the fuel, variability of heat capacity with temperature; non-adiabatic condition of the cylinder, and frictions appear to be the most impactful [9].

Several fuels can be used in ICE, which can be subdivided over two families: organic and inorganic compounds. A further subdivision can be made within the first group by identifying other subcategories: hydrocarbons of natural and synthetic origin (i.e., benzine, diesel, methane, LPG); other organic compounds (e.g., alcohol, biofuel). That subdivision may not be interpreted as a strict categorization into closed boxes since mixtures are often used. For instance, several ethanol mixtures are commonly employed worldwide. Ethyl alcohol is often mixed with gasoline in a weight percentage ranging from 5% to even above 85%. There are also examples of mixtures of hydrocarbons and non-hydrocarbons, such as the hydromethane, called H_2–NG (natural gas) blends or H_2–CNG (compressed natural gas) blends [10]. Both pure and mixed hydrocarbon fuels produce emissions during the combustion process, such as CO_2, CO, C_mH_n, H_2O, NO, NO_2, SO_2, and particulate

matter (PM), according to their chemical composition and reaction with air [11]. Notably, the combustion reaction of an arbitrary fuel ($C_aH_bO_cN_d$) and air (i.e., oxygen as the final oxidizing agent, with an assumed nitrogen concentration of 79.05%) is described by Equation (2):

$$C_aH_bO_cN_d + \lambda\ air \rightarrow\ a_1CO_2 + a_2CO + b_1H_2O + b_2H_2 + e_1O_2 + e_2N_2, \qquad (2)$$
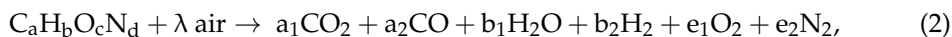
where λ is the excess air ratio (equal to one for stoichiometric reactions and greater for weak mixtures [12–18]) and a_1, a_2, b_1, b_2, e_1, and e_2 are the reaction coefficients. Most of the combustion products—if not all of them—are pollutant emissions. Table 1 lists the main exhaust gases emitted as a result of the combustion process of several fuels and reports their known effects on air quality and human health.

Table 1. Main exhaust gases emitted by conventional combustion processes.

Chemical Species	Pollution Effect
CO_2	Greenhouse gas; according to the available scientific literature, its concentration in the atmosphere is causing climate change [12]
CO	Carbon monoxide; colorless, odorless, and tasteless, but highly toxic; at a concentration greater than 1000 ppm, it is considered immediately hazardous [13]
C_mH_n	For example, benzene (C_6H_6); it damages the bone marrow, depresses the immune system, causes leukemia, and is associated with other blood cancers and pre-cancers [14]
NO_x (NO and NO_2)	NO_x reacts with ammonia, moisture, and other compounds to form HNO_3; it can penetrate deeply into sensitive lung tissue, yielding lung cancer and causing (or worsening) respiratory diseases, which may result in premature death in the worst case [15]
Particulate matter	Better known as PM10 and PM2.5; their inhalation produces asthma, lung cancer, cardiovascular issues, and premature death [16]
SO_2	highly irritating and harmful to the eyes and the respiratory tract; by inhalation, it can cause acute pulmonary edema, with prolonged exposure leading to death [17]
H_2O	Harmless to the environment and human health within a medium-term horizon

As a general observation, ICE has made a breakthrough in human society, both economically and socially. However, the quest for more efficient and environmentally friendly propulsion systems prompted the exploration of different and innovative technologies.

2. Comparison between Electric and Conventional Vehicles

As mentioned in Section 1, electric mobility is the most relevant alternative to ICE towards the reduction of greenhouse gases and pollutant emissions; however, the cost of manufacturing batteries and fuel cells, together with the costs associated with producing and handling hydrogen (e.g., electrolyzers, storage systems) shall be taken into account when assessing their viability. In fact, hydrogen—a viable energy vector—may also be considered promising to balance the intermittent and often unstable availability of numerous renewable energy sources (e.g., solar energy, wind power), thus allowing the fulfillment of the end users' demands over time in terms of electrical power by combining renewable energy and energy conveyed by hydrogen itself [19,20]. Indeed, electric cars are not new vehicles: the first examples were brought to the market in the XIX century, and, in 1900, 34,000 electric vehicles were registered in the USA [11]. They display some advantages as propulsion systems, with respect to ICE:

- Maximum torque can be immediately reached; as a result, acceleration is smoother than that obtained with a traditional ICE, especially those of large size or turbocharged;

- All parts included in a conventional car, such as the engine, radiator, pistons, spark plugs, fuel pumps, exhaust system, and timing belt, are instrumental in performing traction and prone to replacement over time; on the other hand, an electric-powered car presents fewer parts that are potentially replaceable, thus reducing maintenance costs by over 50%;
- All electric cars feature regenerative braking, which employs the electric motor to slow down the vehicle so that some of the power is returned to the battery; therefore, braking is more efficient and also reduces wear by developing less fine dust with consequent savings;
- Electric engines are based on a mature technology, so they allow traveling hundreds of thousands of kilometers without major maintenance [21].

Comparing the travel costs of ICE- and electric-powered cars implies assessing the respective costs against the same distance traveled. Usually, the comparison between spark-ignition and diesel engines is expressed as "liters per 100 km", which indicates the amount of fuel (i.e., liters) required to travel one hundred kilometers (i.e., the same distance traveled). However, the range of electric cars, a famous one of which is shown in Figure 1, is often expressed as energy—the well-known kilowatt-hours—so harmonizing the selected units is much needed to make comparisons.

Figure 1. Photo of Tesla Model S (available online).

Diesel engines feature an efficiency of about 33%, which is essentially the fraction of energy converted into work, with the rest being dissipated in the form of heat. Diesel fuel used in diesel engines generates about 10 kWh per liter; the average range can be calculated by knowing that—considering commonly available price lists—the models on the market present a combined-cycle consumption between 4 and 12 L of diesel per 100 km. Therefore, when running that distance, Diesel cars require between 40 and 120 kWh of energy. On the other hand, spark-ignition engines feature an efficiency of about 28%. Gasoline yields 8.8 kWh per liter, while the average consumption lies between 5 and 15 L of fuel per 100 km. That translates into requiring between 50 and 150 kWh of energy when running that distance. When keeping the same distance traveled, electric vehicles display an average combined-cycle consumption between 15 and 30 kWh. If the average value is considered in the analysis, diesel engines exhibit an average consumption of 80 kWh over 100 km, which is slightly lower than that of spark-ignition engines (87.5 kWh over 100 km); quite remarkably, electric cars exhibit an average consumption much lower than those: 22.5 kWh over 100 km.

As for an economic comparative assessment, the cost per kWh is obtained by relating the average amount of energy required to travel the same distance with the cost of each energy resource employed: 0.14 EUR/kWh for diesel fuel and 0.18 EUR/kWh for petrol. As for electricity, it is necessary to distinguish the supply source instead: supply from a domestic socket (3 kWh with slow recharge) bears an average cost of 0.25 EUR/kWh, while

supply from a fast column implies an increase of up to 0.50 EUR/kWh. Eventually, driving 100 km by a diesel car costs 11 EUR on average, by a spark-ignition car, 16 EUR on average and by an electric car, 6 to 12 EUR, depending on the recharge mode.

Fuel-cell cars, being either FCEV or FCHEV, embody a small yet very particular share of electric vehicles. Although fuel-cell technology is effective in converting chemical into electrical energy and is environmentally friendly, its permeation of the market still appears to be that of a niche. For instance, if focusing on Europe and specifically Italy, fuel-cell cars are in fact a novelty: there is only one currently registered, in Bolzano. That is quite representative of the relationship between the number of cars owned by the population and the availability of the involved fuel: Bolzano is the place where the only hydrogen refueling station is currently operating in Italy. This instance is not merely anecdotal and emphasizes one of the main hindrances against the possibility of spreading fuel-cell cars: the lack of a widespread hydrogen-distribution network. However, there are plans to expand that network almost worldwide—with China ad Europe arguably being at the forefront—which may further the breakthrough of fuel-cell cars on the market. The Italian ENI S.p.A., a multinational energy company, is currently collaborating with automotive manufacturers such as Toyota and Hyundai to build hydrogen refueling stations in Rome and Milan, with the aim of reaching 20 refueling locations by 2023. However, another problem hindering the spread of fuel-cell cars in Italy and many other European countries consists of the rather few available models on the market. They are currently two models: the Hyundai Nexo and the Toyota Mirai (Figure 2); their price is also quite high compared to cars of similar size and conventionally propelled: Hyundai Nexo 163 CV costs about 70 k EUR and features a running distance of 800 km with a full tank; the Toyota Mirai Fuel Cell 155 CV costs slightly more than 65 k EUR and features a running distance of 500 km with a full tank.

Figure 2. Photos of the Hyndai Nexo and the Toyota Mirai (available online).

Despite the abovementioned challenges, fuel-cell cars have proven to be a promising alternative to both conventional and electric cars, as they exhibit several advantages: being virtually emission-free, obviously not including potential pollutants emitted when producing hydrogen as a fuel; including fuel-cell stacks that are smaller and lighter than batteries, also being characterized by a longer life cycle; having a refueling time comparable to that of conventional cars—either gasoline- or diesel-fueled—and remarkably shorter than the full recharging time for batteries. On the other hand, fuel-cell cars also have inherent structural limitations. Notably, their overall weight tends to be higher than that of the other types of cars, which is mainly due to the hydrogen storage system included within. This problem also affects the space available in the cabin and trunk. A general comparison between FCEV and BEV in terms of advantages and drawbacks is proposed in Table 2.

Table 2. Advantages and drawbacks of FCEV and BEV.

FCEV		BEV	
Advantages	**Drawbacks**	**Advantages**	**Drawbacks**
Refuelling in 3–5 min	Poor network of distributors	Zero local emissions	Battery life uncertain (5–8 years)
Long distance with a full tank (400–800 km)	High purchase prices and few models available	No CO_2 production	Shorter driving range than other kinds of cars
Higher energy input of Li batteries	Transformation, transport, and storage still not very efficient	Higher efficiency (reduced losses during transport, storage, and transformation)	Higher production costs
Suitable for heavy transport vehicles (e.g., buses, trucks)	Safety concerns (hydrogen flammability)	Reduced noise pollution	Charging times and car performance not constant
No harmful emissions	Non-environmentally friendly hydrogen production from fossil fuels	Less impactful engine maintenance	Additional costs of rental and ownership
Possible reductions in taxes		Larger availability of charging stations, Electric-motor charging sufficient for urban driving cycles	Inefficient battery recycling technologies

It is worth noting that production costs, manufacturing included, are also currently rather high, as a result of the small segment where fuel-cell cars stand within the market: economies of scale are somewhat yet to achieved. To better understand the difference in terms of driving range and cost, Table 3 shows a comparison between actual FCEV, BEV, and vehicles with traditional ICE. It is apparent that the cost of FCEV is about double that of traditional cars, featuring about the same power. On the other hand, BEV stands somewhat in the middle in terms of cost, even if their driving range is significantly lower than that featured by the other two types.

When considering the comparison between fuel-cell cars and conventional ones, one of the most remarkable advantages of the former consists of their relatively low energy consumption, in addition to being environmentally friendly. As an order-of-magnitude figure, fuel-cell cars consume about 1 kg of hydrogen gas every 100 km. For an analysis that encompasses the economical aspect, it is necessary to compare this consumption with that of a conventional car, for instance, a spark-ignition one: a Fiat 500, one of the models featuring the lower fuel consumption, consumes 3.8 l of petrol every 100 km. Another piece of information may be included in the comparison: the current average cost of hydrogen is 10 EUR/kg, which corresponds to an expense of 0.1 EUR/km. On the other hand, the current average cost of petrol is about 1.5 EUR/L; therefore, a conventional car exhibits a fuel cost of 0.06 EUR/km, which is not dramatically lower than that of a fuel-cell one. It is worth remarking that the whole hydrogen technology (e.g., production, distribution) will likely become more spread and more cost-effective in the near-to-medium term, thus making the hydrogen cost decrease and fuel-cell cars more affordable over their lifetime.

Table 3. Comparison between FCEV, BEV, and traditional cars in terms of driving range and cost (reported data available online).

Propulsion	Model and Power (kW/CV)	Driving Range (km)	Cost (kEUR)	Cost per Unit of Power (EUR/kW)
FCEV	Hyundai Nexo, 120/163	800	70	583
	Toyota Mirai, 114/155	500	65	570
	Honda Clarity FC, 130/177	500	60	461
BEV	Dacia Spring, 48/65	220	21	437
	Fiat 500e, 70/95	300	27	386
	Tesla Model 3, 239/325	491	45	188
	Volkswagen ID.3, 150/204	422	40	267
ICE	Hyundai i20 1.0, 88/120	800	24	273
	Toyota Land Cruiser, 150/204	800	57	380
	Volkswagen Golf 2.0 TDI 110/150	1000	36	327
	Dacia Sandero, 49/65	1000	13	265

In summary, the initial and operating costs of fuel-cell cars are heavily impacted by the methodology for producing hydrogen and the challenges in storing and transporting it, together with the costs associated with manufacturing fuel cells and the components included in a fuel-cell stack. As a hint at a potential further analysis of the impact and costs of hydrogen production, the three well-known routes—green, blue, and grey [22]—to separate hydrogen from other substances represent a categorization in that regard. Notably, producing hydrogen without releasing any pollutants (e.g., carbon dioxide, carbon monoxide) makes it "green": it is very environmentally friendly, but associated costs are higher. On the other hand, separating hydrogen from hydrocarbons (i.e., "grey" hydrogen) is the most cost-effective approach, yet it is environmentally more damaging. However, if the carbon released through grey-hydrogen production is subsequently captured ("blue" hydrogen), costs rise, but the related environmental impact is reduced.

3. Hydrogen Supply and Associated Costs

3.1. Production

Technologies for hydrogen production from several sources have been in use for more than 40 years and more than 90% of them exploit fossil fuels [23]. The current challenge consists of developing techniques that process renewable sources to extract hydrogen without emitting pollutants. Unfortunately, about 68% of the hydrogen currently produced worldwide is separated from hydrocarbons, with natural gas being the most popular (48%), followed by oil (20%); however, most of that hydrogen is consumed internally within oil refineries [24]. Hydrogen production processes are manifold, and, as shown in Figure 3, they can be divided into two main categories: conventional technologies relying on fossil fuels and renewable technologies. Notably, the former processes fuels obtained from fossil-based waste and basically consists of the reforming and pyrolysis of hydrocarbons [25]. In this category, the most renowned are steam reforming [26], partial oxidation [27], gasification [28], and electrolysis [29], if the energy required to operate the electrolyzer is provided by conventional plants. On the other hand, the renewable production category includes a variety of sources: biomass [30], and indirect production from nuclear [31] and natural

energy sources such as wind, sun, and water (i.e., hydroelectricity) [32], with the electroly-
sis sustained also falling within this category. If biomass is considered as a raw material,
other subcategories may be distinguished, such as thermochemical [33] and biological [34]
processes. Thermochemical technology mainly involves pyrolysis [35], gasification [36],
combustion, and liquefaction, while the main biological processes are direct and indirect
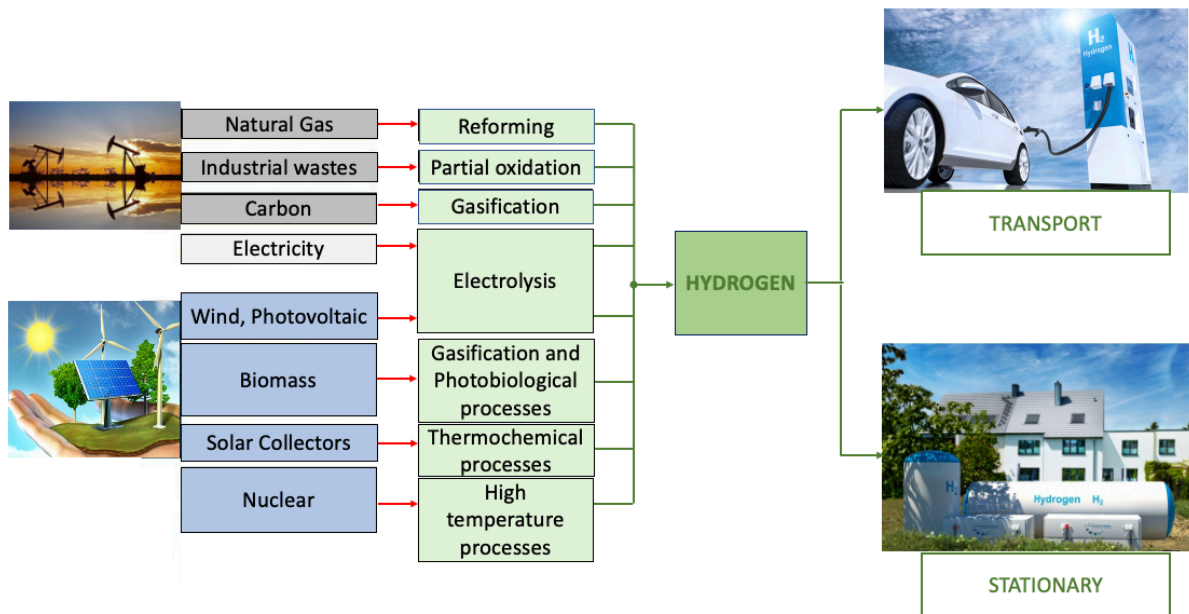bio-photolysis [37].

Figure 3. Main methods for hydrogen production.

Figure 4 shows a comparison of the theoretical (i.e., standard enthalpy of the reaction)
energy spent to produce hydrogen from different sources. It is worth noting that hydrogen
production from light hydrocarbons implies consuming a generally lower amount of energy,
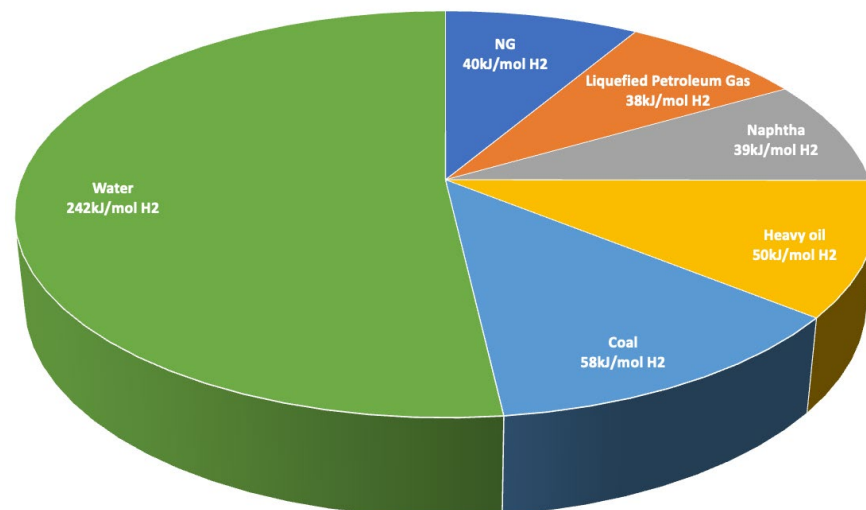while electrolysis requires a bigger quantity and is the most energy-intensive process.

Figure 4. Comparison among different sources in terms of energy demand.

As another comparison among extraction methods from fossil fuels, Figure 5 shows
the stoichiometric efficiency of hydrogen production by gasification of natural gas, LPG
(liquified petroleum gas), naphtha, heavy oil, and coal. The general rule to assess hydrogen
yield implies that as the hydrogen-to-carbon ratio in the hydrocarbon molecule increases,

production efficiency grows, while CO_2 production decreases. This simple outcome from chemical formulations supports the use of light hydrocarbons for hydrogen production rather than heavier hydrocarbons, limiting the associated pollutants emitted.
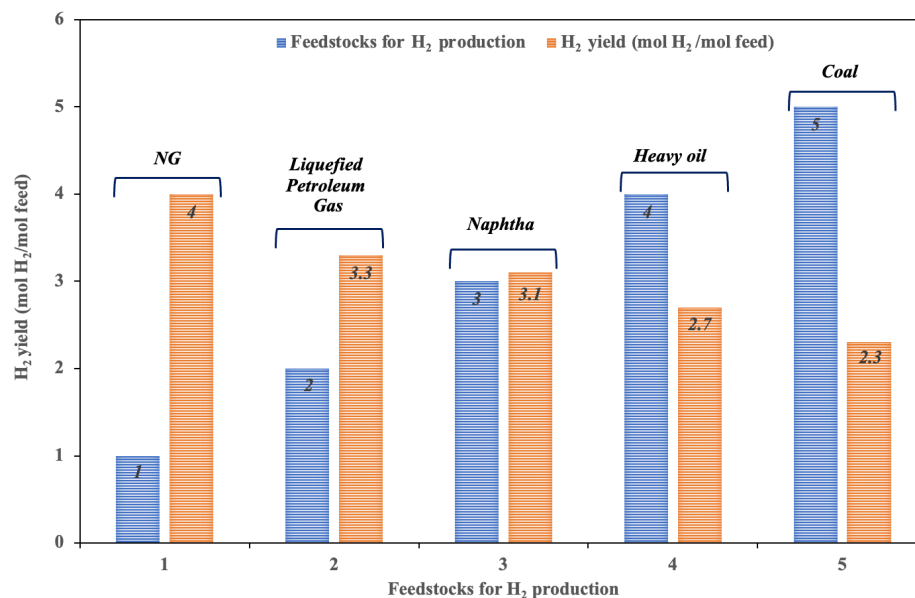

Figure 5. Energy demand comparison among different sources.

It is also interesting to discuss a comparative assessment of the hydrogen production methods in terms of costs, which is reported in Table 4. As expected, steam reforming still appears to be the most cost-effective approach, since its production rate is high (Figure 5) and the associated cost is remarkably low. For the sake of comparison, biomass gasification and pyrolysis are slightly less expensive, yet their yield is significantly smaller, which makes biomass viable only if a large amount of it is available. On the other hand, electrolysis fed by renewable sources bears the inherently high costs related to the latter, while nuclear-sustained electrolysis exhibits remarkably lower costs.

Table 4. Hydrogen production costs.

Source	Production Rate (kg/day)	Cost (EUR/kg)
Nuclear (electrolysis)	1000	3.83
Solar thermal	1000	6.46
Solar PV (electrolysis)	1399	21.48
Wind (electrolysis)	1000	5.12
Biomass (gasification)	194,141	1.33
Biomass (pyrolysis)	72,893	1.36
Coal gasification	281,100	1.15
Natural gas (steam methane reforming)	236,239	2.29

Evaluating production costs may not be disconnected from the analysis of the toxic or harmful byproducts (e.g., CO_x, NO_x) that each considered technique brings. When combining economic and environmental aspects, conventional methods of processing fossil fuels appear to be disadvantageous since CO_2 emissions from the reforming process, coal gasification, or hydrocarbon pyrolysis imply either pollution, or expensive recovery procedures that yield a consequent increase in the hydrogen-production costs. That reason makes coal-gasification technologies—even though at a high readiness level—not at the forefront: their yield is not particularly high (Figure 5), so the environmental concerns related to high CO_x production rise; moreover, the production costs are not so much lower than those associated to methane reforming (Table 4) as to make the former technology

particularly cost-effective. However, the dataset reported in Table 4 may require updates in the near future, thus impacting on the analysis of future energy scenarios: the possibility to have low-cost hydrogen production from renewable sources is becoming more likely, which may also suggest reconsidering the option of coal hydrogasification. Coal represents a sort of large reservoir of low-cost energy and could support the development of emerging countries in a medium-term horizon, simply by fostering hydrogen economy. However, coal is the fossil fuel that produces the highest greenhouse gas emissions, and therefore its use shall be accompanied by subsystems that allow implementing the reduction of its environmental impact (e.g., carbon sequestration) and increase its social acceptability.

Summarizing the current energy scenarios and highlighting their potential futures, on the one hand, it appears that steam reforming of light hydrocarbons (i.e., natural gas) still appears to be the most cost-effective and least polluting hydrogen-production technique among the traditional, non-renewable ones. However, the large availability of coal may make it a promising low-cost source. A wider penetration of renewable hydrogen production is also expected, which, however, would require a reduction of the costs associated with electrolyzers and the renewable sources used to feed them (e.g., solar, wind), or large amounts of biomass to sustain a poorly yielding technology. As for nuclear power employed to supply the energy required for electrolysis, the current concerns on nuclear energy (e.g., management of nuclear waste, safety requirements) may or may not act as a hindrance against this approach in the future.

3.2. Storage

As remarked in Section 2, the hydrogen cost does not depend only on the current production techniques, but also on the storage technologies. To be directly available to end users, hydrogen has to be properly stored and transported in its different possible phases: solid, liquid, or gaseous. To date, this challenge embodies one of the most significant problems to be solved towards a transition to a hydrogen-based economy [38]. From a gravimetric standpoint, hydrogen is the substance that allows the best ratio between stored energy and weight. On the other hand, in standard conditions, the energy-to-volume ratio is not favorable at all. The US Department of Energy (DOE) established that hydrogen can be considered an acceptable fuel when its energy density is 6.5 wt% of the total weight of the tank, which must contain 62 kg/m^3 of hydrogen [39,40]. DOE targets are summarized in Figure 6 for all the classes of materials involved.
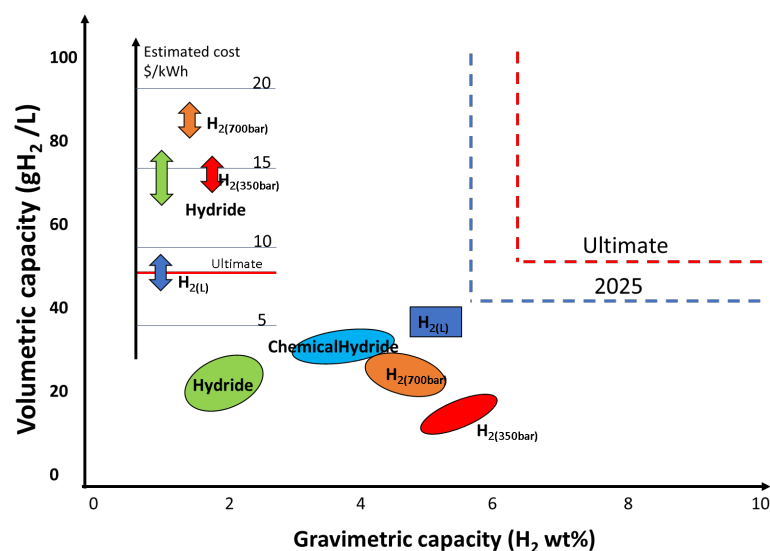

Figure 6. US DOE targets for hydrogen storage in terms of gravimetric and volumetric capacity [40], together with the current situation of the available storage strategies.

Overall, the most common and widespread storage method is hydrogen compressed in pressurized tanks as a gas. In addition to that, liquid hydrogen is also adopted as a storage strategy, provided that thermally insulated tanks be employed to avoid evaporation by heat transfer with ambient air. A novel and promising technology consists of the adsorption—either physical or chemical—of hydrogen molecules into solid nano-porous matrices at a generally low temperature and pressure close to the atmospheric value. The whole assembly is in the solid phase, with hydrogen combining with other compounds, thus yielding simple or composite metal hydrides; as opposed to the other two more conventional methods (i.e., gas and liquid), no extreme conditions in terms of temperature and pressure are featured in hydrides, with both being close to standard.

As previously remarked, hydrogen is mostly stored and transported as a compressed gas; unfortunately, it also appears to be the least effective method, as is apparent in Figure 6 [40]. A typical industrial steel tank (50 L volume) can contain an amount of hydrogen of about 0.9 kg, with storage pressure of 200 bar (recently, storage pressure has reached over 350 bar). It is worth noting that about 10 m^3 of gaseous hydrogen can be stored at standard temperatures and pressures. Increasing the storage pressure up to 700 bar in steel tanks poses some structural challenges and typically results in poor energy density: tank weight and dimensions must increase since a larger thickness of the steel walls is required to support the higher pressure. The most promising solution is to employ and make largely available in the market low-weight and high-strength tanks, often made of composite materials [41]. For instance, fiber-reinforced tanks have recently been developed (e.g., aluminum-carbon made [42]), but their current high cost embodies an implicit surcharge on the overall storage cost, thus making composite materials an even less cost-effective strategy. The associated energy density still remains somewhat low, even though it is higher than that provided by pure steel tanks when storage pressure rises up to 700 bar [43]. If storage is put into the automotive context, it is worth remarking that high-strength steel or other metals are able to guarantee mechanical resistance, but their use on vehicles may cause problems due to the substantial weight associated with those tanks. Tanks made of composite materials (i.e., Al, Fe, or polymers) are then employed for the purpose, thanks to their lower density than that of metals. Their typical storage pressure ranges between 350 and 700 bar. The energy density associated with a 700 bar container for automotive applications is 4.5 wt%, which is close to the aforementioned target set by the US DOE [39,40]. In their most recent prototypes, car manufacturers such as Daimler Chrysler, General Motors, Honda, and Toyota installed tanks with those characteristics; dedicated tests demonstrated their reliability, and some models featuring those tanks have also been homologated in Germany, well-known for its high safety standard. Even if a leakage occurred in such tanks, thus potentially fueling a fire, the associated hazard is smaller than that of gasoline tanks. As an expected outcome, any accidental rupture of a tank containing pressurized hydrogen causes the immediate dispersion of the gas, which makes explosion quite unlikely. On the other hand, fuels such as petrol or diesel, despite being liquid, release flammable vapor, which persists in the region where the release occurs as a result of their relatively high density and may likely lead to an explosion [44].

Another methodology to compress hydrogen consists of electrochemical compression, the system of which is practically a fuel cell that works in reverse mode. The efficiency of such systems is usually higher than that of common mechanical compressors, given the absence of moving parts; electrochemical compressors also benefit from silent operation, thus being almost noise-free [45].

As for hydrogen storage in the liquid phase, the liquid-hydrogen density is obviously much higher than that in the gas phase under standard conditions [46]. Therefore, tanks for liquified hydrogen are not required to withstand high pressure since a considerable mass can be contained at a pressure close to the atmospheric value. Therefore, wall thickness may be reduced with respect to storage as a pressurized gas, thus reasonably achieving a weight ratio that satisfies the target suggested by the US DOE (6.5 wt% [39,40]). Unfortunately, hydrogen liquefaction involves energy consumption of up to 30% to 40% of the intrinsic

energy content of the liquid phase. Furthermore, once liquefied, hydrogen shall be kept at a temperature of about 20 K (critical temperature is 33 K). That means heat exchange with the outer air through the walls causes immediate evaporation, which implies wasting part of the energy used to liquefy. Moreover, evaporation leads to reduced efficiency of the storage system, as part of the contained hydrogen is lost as a gas. This is why thermal insulation is instrumental in achieving the effective storage of liquified hydrogen; a double shell is often provided in the tanks used for the purpose, with liquid nitrogen—indeed, another fluid at very low temperature—is included within the envelope between the internal shell and the external jacket of the tank. However, this structural configuration adds complexity to the whole system, which translates into costs higher than those of a single-layer tank.

As previously mentioned, metal hydrides are becoming an alternative to the more conventional storage methods since they combine the possibility of operating at conditions close to standard and a relatively simple setup. For instance, at cryogenic temperature (70–100 K) and moderately high pressure (1–50 bar), carbon nanostructures can be employed to host hydrogen molecules through adsorption. Among the most promising and investigated carbon structures, nanotubes, nanofibers, and graphene are arguably the most renowned [47]. The chemical reaction describing how a generic metal hydride is formed is reported in Equation (3):

$$M + xH_2 \rightarrow MH_x \ (\Delta H < 0), \tag{3}$$
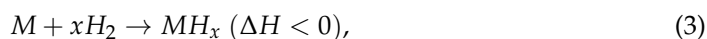
where M is the type of metal or metal alloy capable of reacting with hydrogen, MH is the corresponding metal hydride formed, and ΔH is the enthalpy of reaction. This reaction is reversible: increasing pressure or decreasing temperature implies hydrogen adsorption (i.e., exothermic process), with an equilibrium shifting to the right; increasing temperature or decreasing pressure implies hydrogen desorption (i.e., reverse process, endothermic) through the well-known Le Chatelier-Braun principle [48].

One of the main conditions for the use of metal hydrides for this purpose is their stability during the process of desorption or dissociation of hydrogen. Stable hydrides are generally formed of poorly electronegative pure metals, called "type A metals" (e.g., Li, Na, K, Cs, Mg, Ca, La, Ti, Zr); they exhibit a high dissociation temperature and/or low equilibrium pressure. Among those metals, only magnesium can be potentially employed, since its desorption pressure and temperature are 1 bar and 573 K, respectively. The most electronegative "type B metals", such as Cu, Ni, Co, Fe, Mn, Cr, and Mo, form unstable hydrides with their operating temperatures and pressures being rather high [49]. To benefit from the characteristics of both classes of metals, mixed classes of compounds are also being considered, which are called intermetallic type AB [50]. Various combinations of metals belonging to the two classes have been and are still being investigated. Table 5 reports some of the metal hydrides that are proven effective in hosting hydrogen under a pressure condition (1 bar) close to atmospheric [51,52].

Table 5. Summary of largely available metal hydrides with their characteristics.

Metals	Type	Hydrides	H$_2$ Capacity (wt%)	T (K)
Mg	A	MgH$_2$	7.60	552
MgTi	AB	FeTiH$_2$	1.89	265
ZrMn$_2$	AB2	ZrMn$_2$H$_2$	1.77	713
Mg$_2$Ni	A2B	Mg$_2$NiH$_4$	3.59	528
LaNi$_5$	AB5	LaNi$_5$H$_6$	1.37	285

Other types of complex hydrides are available, such as NaAlH$_4$ or NaBH$_4$, which are capable of reaching and exceeding the storage of the liquid phase (over 7 wt%) [53]. These complex hydrides can return hydrogen under temperature and pressure conditions, which is not too different from standard. When referring to this storage method in automotive applications, it is worth noting that hydrogen is made available by desorption directly on

board, without requiring a massive storage volume, since volumetric capacity tends to be higher than that of conventional storage systems (Figure 6). The main drawbacks consist of the relevant initial cost of the involved materials, approximately equal to 50 times the energy equivalent in gasoline. Moreover, the desorption cycle is practically irreversible since reobtaining $NaBH_4$ after desorption would entail too much energy consumption.

In all the conventional storage methods reviewed here (i.e., compressed, and liquefied hydrogen), hydrogen distribution in pipelines requires the use of mechanical or electro-chemical compressors [45]. Some types of metal hydrides are an exception in that regard since their pressure plateau is relatively low. The cost of compressors depends on the inlet and outlet pressure and the operative flowrate. The most common are reciprocating compressors, which cost between 650 and 6600 USD/kW [54]. Their unit cost is inversely proportional to their dimensions: the larger they are, the higher the savings on the unit cost. It is worth remarking that liquid-hydrogen storage also depends on the amount of hydrogen released per hour, with the price ranging from about 25,600 to 118,000 USD/(kg h) [55]. On the other hand, the purchase cost of metal hydrides includes not only the metal-alloy assembly but also the vessel containing it and an integrated heat exchanger, which is necessary during both the absorption (i.e., heat removal) and the desorption (i.e., heat supply) phases. Some metal hydrides also require high operative pressure, which implies the use of a compressor. Their unit cost for processed hydrogen ranges from 820 to 60,000 USD/kg [56].

3.3. Distribution

Hydrogen distribution is of paramount importance, as remarked in Section 2. However, the selected distribution method mainly depends on the employed storage technique. In general, compressed hydrogen is transported by high-pressure cylinders, tankers, and gas pipelines [57]. Although they are of a relatively small size, high-pressure cylinders are somewhat dangerous and difficult to transport; tankers are the most suitable carriers for hydrogen cylinders, with the latter being made of steel and mounted into protective frames able to host many of them. Each cylinder can contain from 63 to 460 kg of compressed hydrogen at 20 MPa pressure. Tankers can also carry liquified hydrogen. This form is more convenient in terms of transport, as the mass-to-space ratio is higher than that featured by the gaseous phase, thus also increasing the energy capacity of the whole transport system. However, it is inconvenient if the costs associated with maintenance and refrigerating the tank are also included in the overall evaluation. Another major problem consists of transport safety: in the unfortunate event of a road accident, the possible rupture of cryogenic cylinders may cause serious issues, as the employed refrigerant would be released without control. Quite remarkably, rail transport of compressed or liquified hydrogen is not yet carried out, since it would entail a substantial increase in the transport costs due to the need for providing wagons specifically designed with materials suitable for its transport [58]. As for maritime transport, the long-distance journeys involved make it preferable to transport liquified hydrogen to avoid large amounts of high-pressure gas aboard. It is worth mentioning that Canada has developed numerous naval projects for the transoceanic transport of hydrogen. One project involves the use of five small barges carried within a larger ship, which can be separated upon reaching the final destination [59]. Each barge is capable of carrying 21,200 kg of hydrogen.

An innovative technique benefiting from the transport of hydrogen consists of employing a gas pipeline that also contains a superconducting material. Liquid hydrogen would act as a refrigerant for the superconductor and would allow the transport of electricity over long distances, without the substantial current losses typical of conventional power lines. In general, gas pipelines, also known as hydrogen pipelines, are largely used for the purpose of distributing hydrogen. As with every gas, it can be transported in the same fashion as natural gas currently is; however, the materials used to make up the network shall be selected appropriately to address the specific substance involved. Notably, the contact between hydrogen and special steel causes embrittlement, which may lead to a massive increase of leakages and losses. Therefore, it is necessary to carry out an *a priori*

assessment of the piping and subsequently monitor the average flowrate to detect potential leaks that may also be hazardous due to hydrogen ignitability [60–65].

On average, hydrogen pipelines have a 35–50 mm diameter, and gas flows within them at 2–10 MPa pressure. It is worth noting that hydrogen has a volumetric energy density and a dynamic viscosity slightly lower than that of natural gas. So, the energy required for hydrogen pumping is higher, yet comparable to that required to convey the same amount of energy by natural gas. In some pipelines, the hydrogen flows as a liquid, but the conditions at which it must be kept (20–25 K) and the difficulty of selecting appropriate materials able to withstand them make this strategy hardly feasible on a large scale. The existing pipelines for hydrogen, although to a much smaller extent than those for natural gas, are approximately 1000 km in North America and 1500 km in Europe. Large-sized pipes made of standard steel—therefore not subject to specific requirements—have transported hydrogen in Germany since 1938 without any remarkable safety problems. However, those pipes are equipped with sensors for the detection of potential leaks, and periodic inspections are also enforced.

4. Fuel Cell Components

Despite the high expectations surrounding fuel-cell vehicles, especially related to the possibility of increasing running distance in electromobility, the manufacturing and production of fuel cells is still a costly process. The cost per unit of power generated by fuel cells is estimated to drop by a factor of ten, as this technology is expected to increasingly penetrate the market. The high costs are mainly due part to the materials involved, such as the Nafion membranes and the Pt-based electrocatalysts [66], and the manufacturing techniques employed; however, the transition from small batches to large-scale production has not been completed, which would in fact allow benefiting from an economy of scale. Market surveys show that with a production rate of over 100,000 pieces per year, materials procurement costs are typically cut by more than 70% compared to a production rate of 100 pieces per year. A further reduction in costs may be yielded by new materials, which is the main motivation for research in that realm. Overall, the quest for more cost-effective solutions for each component of the fuel-cell stacks is still ongoing. As mentioned in Section 1, PEMFC is the fuel-cell type most employed—if not the only one—in the automotive sector; as expected, it is also the type bearing the lower associated costs, thanks to its low-temperature operation that leads to relatively minor stress on the materials.

Over the past decade, fuel cells have exhibited a general improvement in terms of system performance. World-renowned car manufacturers, such as Daimler Chrysler, Honda, Hyundai, and Toyota, have recently developed a new set of fuel-cell cars that can match the characteristics of spark-ignition and diesel cars in terms of speed, acceleration, and running distance with a full tank. This step forward was made possible by the advancements achieved both on fuel cell components and on the entire system, with durability and reliability standing out as the most improved aspects. While material properties determine the power density of fuel-cell stacks, on the other hand, the arrangement of the systems, the thermal management of the whole assembly, the fluid circuit, and the control strategy determine the driving conditions.

4.1. Proton Exchange Membranes

Usually, the solid PEMFC differ from other cells known as high temperature PEMFC (HT-PEMFC): the main difference between those two categories of the same fuel-cell type, apart from operating temperature, consists of the different type of proton exchange membrane included within the MEA (membrane electrode assembly). The well-known membrane material for PEMFC includes a PTFE (polytetrafluoroethylene) backbone, where a perfluorovinylether side chain binds a sulfonic acid group. These kinds of commercial standard membranes, mostly named Nafion, Flemion, or Aciplex, have an equivalent weight of 1100 g/eq. As reported in Table 6, the condition leading to the best performance in terms of proton conductivity is an operating temperature of 80 °C, as a maximum proton

conductivity of 0.1 S/cm is reached. It is also necessary that hydrogen be saturated with steam before being supplied to the cell at the anode site to prevent the Nafion membrane from drying out. This step is of paramount importance because the proton transport mechanism—either vehicle or jump mechanism—through the membrane relies on water as a vehicle for protons. On the other hand, the opposite problem to PEMFC dehydration also occurs and consists of flooding of the outlet cell. To address those two issues, several strategies have been pursued to improve water management in fuel cells. Among them, the use of a porous septum in the electrolyte appears promising [67], together with a modification of the geometry of bipolar plates [68]. However, to date, the most beneficial approach is the humidification of the reagent gases [69]. Past works [70] show that an optimal range of humidification of the gases entering the cell lies between 40% and 70%.

Table 6. Nafion membranes (*RH* stands for relative humidity).

Nafion Type	Maximum Power Density (W/cm^2)	Current Density (mA/cm^2)	Operative Conditions	References
Nafion HP	2.28	~5000	H_2/O_2; 90% RH; 100 °C	[71]
Nafion 211	0.6	1250	H_2/air; 96% RH; 70 °C	[72]
Nafion NR211	0.98	1500	H_2/O_2; 100% RH; 80 °C	[73]
Nafion 212	0.9	2250	H_2/O_2; 100% RH; 80 °C	[74]
Nafion NE1035	1	2000	H_2/O_2; 100% RH; 70 °C	[75]
Aquivion E87-05S	1.1	2500	H_2/O_2; 60% RH; 120 °C	[76]
Nafion 117	0.4	784	75 °C/95% RH	[77]
Nafion 112	0.5	1041	90 °C/95% RH	[78]

Although operating PEMFC at a high temperature can rule flooding out, that would lead to detrimental membrane dehydration and to a substantial loss of ionic conductivity. Several kinds of Nafion membranes are currently available, which differ in equivalent weight, thickness, and other properties. Each displays various values of performance indexes; Table 6 reports the maximum power density as the most significant one.

Conductivity of membranes is strictly dependent on the equivalent weight of the polymer; for instance, in a polymer featuring a high equivalent weight, conductivity drastically decreases with the relative humidity of the reacting gases: from 100% to 25% RH, the decrease is higher than an order of magnitude [79]. Despite the fact that membrane conductivity increases with temperature, it was found that at a 120 °C operative temperature and 25% RH, it cannot reach the target value. This condition has further promoted studies of proton-exchange polymeric membranes able to operate in low humidification conditions. The new developed membranes are also expected to have lower cost and higher durability than those currently on the market [80]. With reference to the automotive sector, the cost of the membrane amounts to about 30–40% of the total cost of the fuel-cell stack [81].

The most studied membrane classes include PFSA (perfluorosulfonic acid) membranes with low equivalent weight. They are composite membranes, developed by adding metal oxides into the polymer matrix, such as SiO_2, ZrO_2, Al_2O_3, TiO_2, clays (montmorillonite), zeolites, heteropolyacids, and zirconium phosphates (ZrP) [82,83]. These chemical components have the main function of keeping the absorption of water as high as possible at a high temperature and low humidity, as well as increasing the mechanical stability of the membrane itself. The inorganic/organic filling material can improve water absorption through its hydrophilic groups by reducing the water transfer into the membrane, while

simultaneously increasing proton conductivity. Since inorganic nanoparticles also act as a mechanical barrier, it is worth establishing the most effective amount of material to add to the polymeric matrix to prevent reduction of proton conductivity [84]. Another class of widely studied materials is the family of aromatic polymers, such as sulfonated polyether-ketones (SPEK, SPEEK, SPEEKK, and SPEKEKK [85]) and sulfonated polysulfones [86], which show high mechanical and thermal stability at high temperatures, together with conductivity comparable to that of the commercial Nafion membranes and are also low cost. However, the limitation of these membranes consists of the need for hydration to achieve high proton conductivity, which is indeed a major limitation to overcome. Other types of developed membranes are acid-base polymers. The use of nonaqueous solvents as proton carriers in place of water and solid-state materials as proton-conducting media has been at the forefront of research. As another potential breakthrough in membranes for PEMFC, one of the most relevant acid-based polymeric membranes is phosphoric acid-doped polybenzimidazole (PBI) [87]. In fact, the proton conductivity of PBI is quite low, so doping substances such as sulfuric acid, nitric acid, and phosphoric acid, are used. Phosphoric acid exhibits many advantages in terms of stability with respect to other acids. However, the phosphoric acid loss rate during cell operation should be minimized, and the doping level of phosphoric acid should be optimized to emphasize proton conductivity and mechanical stability.

4.2. Electrodes

The MEA of a fuel cell comprises the membrane, at least in the case of the solid bodies involved, as in PEMFC, and the electrodes, with the latter being the anode and cathode. As shown in the generic sketch presented in Figure 7, the polymeric membrane physically separates the anode from the cathode. The electrodes are typically porous and impregnated with platinum that acts as a catalyst for the reduction/oxidation reaction occurring between hydrogen and oxygen. The external surface of the electrodes is made water-repellent by applying a Teflon-coating that allows diffusion of the incoming and outgoing gases to and from the electrodes, while also keeping water in contact with the membrane [88]. The electrodes are basically an interface between the reacting gases and the electrolyte, so they should allow permeation of moist gas, provide a reaction layer anywhere they are in contact with the electrolyte, and finally be conductive: conduction of the free electrons made available by the reaction has to flow from the anode towards the cathode. The materials complying with these requirements are carbon fibers, thanks to their porosity, water-repellent nature, conducting nature, and corrosion resistance. Furthermore, they can be assembled in a very thin structure that maximizes the transport of gas and water.
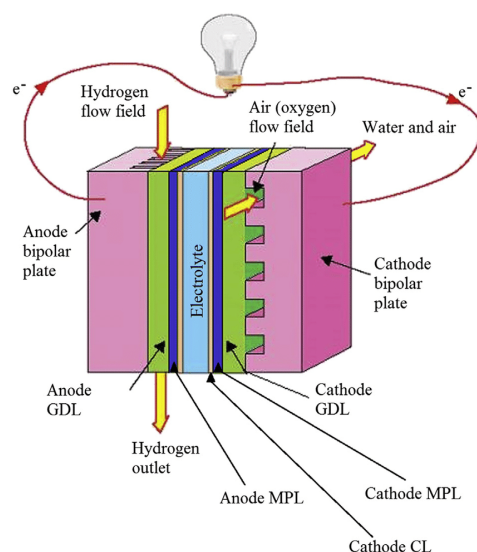

Figure 7. Sketch of a generic PEMFC, with MEA and additional components.

Figure 8 shows a schematic configuration of a fuel-cell electrode, highlighting the interphase and interface between the electrolytic component and the electrode ones (i.e., the diffusion layer of the reagent gases and the electrocatalyst). The catalyst (e.g., Pt), reduced to nanometric dimensions, can be efficiently dispersed on and within the carbon substrate, thus reducing the load of such critical raw materials down to a few milligrams per unit area.
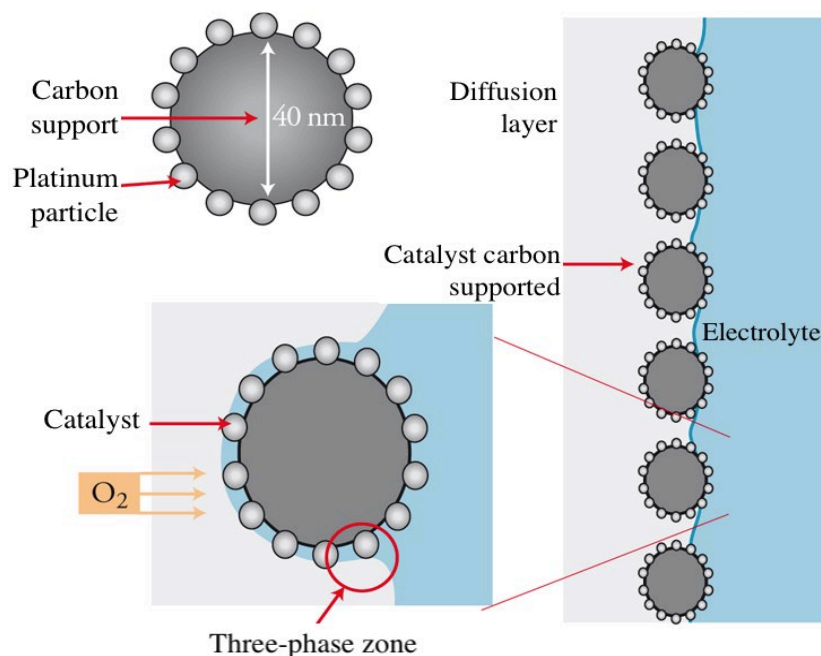

Figure 8. Electrode configuration.

The reactions at the electrodes do not occur spontaneously; catalysts are instrumental in making them take place by lowering activation energy. A well-known electrochemical concept, the forward reaction, is favored when production of electrons and therefore of electric current is as fast as possible, with the voltage between the electrodes not being too low. The high initial cost of the catalyst layer embodies one of the main challenges hindering PEMFC commercialization. Notably, it is closely related to the low stability and high cost exhibited by the electrocatalysts used for the oxygen/air reduction reaction at the cathode and the oxidation reaction of hydrogen at the anode [89].

4.3. Electrocatalysts

As recalled in the previous section, to favor the reactions at the electrodes and accelerate their kinetics, it is necessary to resort to applying catalysts at those sites since the electrode processes, such as the oxidation of hydrogen and the reduction of oxygen, proceed through adsorption/desorption phenomena on a solid substrate. Notably, the substrate is where hydrogen or oxygen releases or receives electrons. In the hydrogen oxidation reaction, the process can be assumed to take place through a sequence of steps, which initially involve the transport of a hydrogen molecule from the gas phase onto the solid substrate and its adsorption on the surface; this stage is followed by the electrochemical oxidation of the adsorbed hydrogen and, finally, by the release of the formed species into the electrolytic phase. The oxygen reduction process is even more complex since it involves several parallels and consecutive steps, including hydrogen peroxide as an intermediate product. Therefore, the speed of the electrode processes is affected by the substrate nature, particularly by the value of hydrogen or oxygen adsorption enthalpy. As a straightforward consequence, the kinetics of the electrode processes can be accelerated, thus reducing the undesired overvoltage at both electrode sites by selecting the most suitable substrate. More specifically, the substrate acts as a catalyst for whichever electrode reaction. The most effective catalysts for the hydrogen oxidation process are noble metals,

such as platinum, palladium, or ruthenium, while for oxygen reduction, in addition to platinum and palladium, nickel and its oxides can be used if the operative temperature is sufficiently high.

To date, the most used electrocatalysts for PEMFCs are Pt-based, with platinum being well-known as a noble metal with a significantly high cost. Other materials (e.g., nickel, palladium, cobalt, silver) may also be used, even though their impact on reaction kinetics is relatively less favorable than that of platinum [90]. The catalyst is added to the surface of each electrode on the side where it is in contact with the electrolyte. Notably, it is bonded to carbon powder, with the latter having an average particle size in the order of 10 nm. Platinum particles have a characteristic diameter of 2–3 nm and are adsorbed within the solid mixture. To be truly effective, the Pt/C powder should be also intimately mixed with the ionomeric form of the polymer membrane to ensure adequate ion conduction between the catalytic layer and the membrane itself. Therefore, the electrocatalyst is actually composed of a mixture of Pt/C/ionomer and each of the three components is uniformly distributed in the catalytic layer. If the cell is fed with hydrogen obtained from hydrocarbon reforming, the fuel may not be pure: even a small fraction of carbon monoxide (usually greater than 10 ppm) is sufficient to poison the active sites of the catalyst. This undesired mechanism is due to the strength of the Pt-CO bond being greater than that of the Pt-H bond: carbon monoxide can bond tenaciously with platinum, thus preventing the adsorption of hydrogen and ultimately leading to rapid degradation of cell performance.

As promoting the anode reaction is arguably most in-demand since hydrogen is involved at that site, the requirements for an anodic electrocatalyst can be summarized as follows:

- High activity in hydrogen oxidation, even at low catalyst loading (0.1–0.3 mg/cm^2);
- Tolerance to carbon monoxide in a concentration ranging between 10 and 100 ppm;
- Stability in the selected operating conditions;
- Low cost.

To reduce the cost associated with the catalysts and therefore the total cost, two possible strategies have been explored over the last three decades. The first consists of reducing the platinum load, whereas the other is replacing platinum with non-noble metal catalysts [91]. As reported by an analysis of the National Renewable Energy Laboratory (NREL) [92], until 2008, the cost reduction in fuel-cell manufacturing achieved was almost entirely related to the reduction of platinum loading down to 0.25 mg/cm^2, with this assessment being based on the platinum cost of USD 1.100 per 31.1 g.

A distinction exists between catalysts formed with a low platinum content and Pt-free hybrid catalysts. The latter do not exhibit sufficient stability yet, so the comparison with Pt-based catalysts appears penalizing; however, catalysts with low platinum content require lengthy activation (longer than 10 h). It is known that Pt-based catalysts show remarkable capability of dissociating the highly corrosive and harmful peroxide intermediate for PEMFC. Therefore, the interaction between Pt-based catalysts (including platinum-group metals, PGM) at low platinum concentrations and PGM-free catalysts yielded encouraging results [93].

Notably, the interaction between a noble metal and a non-noble metal belongs to the core-shell type: the outer shell is made of the noble metal, while the core is made of a non-noble metal. Among the catalysts used, the core-shell, noble metal-based structural nanomaterials are the most promising. The main advantages consist of employing a relatively inexpensive material in the core, which acts as a support for the noble metal in the outer layer, and reducing the cost associated with preparing the catalyst. Moreover, improvements in the catalytic activity and higher stability appear to arise in a particularly complex reaction environment. From previous studies, this benefit is related to multiple factors, such as the bond between the two metals that leads to a structural variation with electron transfer in the core-shell area; the effect of deformation caused by compression of the noble metal shell lattice that creates a change in the surface adsorption energy; and variation of the three-dimensional atomic structure on the surface that governs electrochemical

properties [94]. As a distinctive example in the automotive sector, a PtCo/C-based cathodic catalyst is used in the fuel-cell stack of the Toyota Mirai. PEMFC performance has been significantly improved in recent years by using a PGM-free cathode, thus approaching the suggested targets in terms of power density and efficiency. However, durability is still a major challenge. Moreover, a phenomenon directly impacting on the amount of catalyst in the electrode and ultimately the stack cost is mass-transport resistance, which is emphasized in the proximity of the platinum layer due to the thin polymer layers of the ionomer [95]. Among the non-noble metal catalysts, some show good catalytic behavior, high stability in acid solutions with anodic potential, and resistance to CO poisoning [96,97]; they include carbides of the molecular complexes of macrocyclic transition metals belonging to the IV—VI groups, such as tungsten carbide [98].

4.4. Additional Components of the Membrane Electrode Assembly (MEA)

In addition to the polymeric membrane of PEMFC, MEA also consists of a gas diffusion layer (GDL) and catalyst layer (CL), as included in the sketch of Figure 7. The performance of electrodes—even featuring high catalytic activity—strongly depends on the electrode structure. The removal of water formed through the involved electrochemical reaction is a significant target; to this end, the gas diffusion layer (GDL) plays a crucial role in the water management of any fuel-cell type. Macro-porous GDL, with thickness between 200 and 400 mm, are typically coated with a microporous layer (MPL, 30–50 mm thickness), which facilitates the transport of gas and electrons. GDL is usually made of carbon, water, alcohol, and a hydrophobic substance such as polytetrafluoroethylene (PTFE) that is aimed at promoting gas and water transport in flooding conditions [99]. While a certain thickness is required for GDL to distribute gas in the horizontal direction (i.e., the direction perpendicular to the membrane surface, from left to right, and vice versa, in Figure 7), the microporous layer facilitates the removal of the produced liquid water, thus preventing the undesired flooding of electrodes. It is worth noting that the effective prevention of such flooding can significantly increase cell voltage. As for the GDL cost, the most acknowledge reference consists of the assessment of the stack employed within the Toyota Mirai propulsion system [81], which features a net power slightly lower than 100 kW (370 cells, with total active area of about 9 m^2). The total associated cost ranges from above 80 to less than 40 USD/kW, when annual production raises from 200 to 1000 stacks. An increase of 1.00–1.50 USD/kW applies to those amounts if hot pressing of the GDL onto the MEA is taken into account. The impact of GDL cost on the total cost of the fuel-cell stack (e.g., about 170 USD/kW in the case under consideration, with 1000 stacks produced per annum [81]) results in slightly lower percentage than 15%.

The other MEA component is CL, where the electrochemical conversion reaction of hydrogen and oxygen into water and electricity occurs. CL has a porous structure, with porosity ranging between 40% and 70%; the catalyst, with particle size varying from 1 to 10 nm, is dispersed within this layer. The thickness of the full CL is in the order of 5–100 μm [100]. The costs associated with CL production may take several parameters into account, including the platinum cost—inherently variable over any considered timeframe—and the manufacturing cost. If the catalytic ink is deposited by slot-die coating—one of the most popular techniques in mass production—the manufacturing cost is about 2 USD/kW, with the total cost, materials and manufacturing included, in the 70–80 USD/kW range [81]. This amounts to about 40% of the total cost of the fuel-cell stack.

Substantial research on different types of MEA is ongoing and promising results have been achieved in relation to the main challenges, including performance, lifespan, and cost reduction. One of the areas where most improvements have been recently proposed is the gas diffusion electrode (GDE). The most crucial step when preparing a GDE is depositing the required amount of the catalyst at each relevant location onto the layer, thus limiting any waste of raw materials and making associated costs decrease [101]. To this end, 3D printing has recently demonstrated its potential [102–104], also benefiting from applying a consolidated approach (e.g., extrusion) to additive manufacturing [101,105,106].

Among the large-scale GDE manufacturers, Gaskatel is one of the most renowned [107]; however, many other companies (e.g., Fuel Cell Store and Fuel Cells Etc.) produce GDE upon request—both small and massive batches—also allowing to vary dimensions, type of catalysts and their amount and concentration in the catalytic layer.

As another type of MEA currently on the market are catalyst coated membranes (CCM). Among the most employed and effective methods to prepare CCM are ultrasonic spray atomization and inkjet printing [108–111]. MEA, prepared by those techniques, exhibits a higher performance level, compared to other techniques employed in the past (e.g., spin coating); they provide lower electrical resistance, emphasized proton transfer and reduced amount of platinum required. The last feature is obtained, thanks to deposition being more homogeneous, with consequent reduction in production costs. This type of MEA is being developed on a large scale by various companies, such as Johnson Matthey, Ballard, 3M, Gore, and Toray.

4.5. Bipolar Plates

The component having the most significant impact on weight and volume of a fuel cell is the gas-flow plate, also known as bipolar plate (Figure 7), the purpose and features of which are very important, as they allow assembling a stack of single cells connected in series with each other. Therefore, electrical, and thermal conductivity of this component are characteristics instrumental to achieve high performance of the whole stack. For the same reason, resistance to electrochemical corrosion is also of paramount importance. Moreover, they shall allow a homogeneous distribution of hydrogen at the anode and of oxygen at the cathode, thus preventing dangerous hot spots from occurring, which consist of locations where higher current density arises, thus consequently yielding a major possibility of damage for the cell.

Graphite is the most used material in producing bipolar plates, thanks to its hydrophobicity, low corrosion, high electrical conductivity, and relatively easy machinability. Metals, such as aluminum, exhibit an even higher conductivity and are also manageable in the manufacturing stage, but feature poor corrosion resistance, thus requiring treatments with anti-corrosion paint to prevent their deterioration. Currently, the preferred material is a composite made of a graphite/polymer blend. Although it shows conductivity slightly lower than that of pure graphite, it exhibits greater strength and flexibility; therefore, it allows constructing plates with minimal thickness. Ultimately, that yields a remarkable reduction in weight and volume of the cell. One of the main advantages of these composite materials consists of the possibility of manufacturing through injection-molding technique [112]. Another material used for the same purpose is steel, with which extremely thin layers can be manufactured, and also benefits from mass-production techniques typical of that material [113]. Another type of material used to make the plates is a mixture of graphite and metal powder, the structure of which is porous with an average pore diameter of about 10 μm [114]. Another type of bipolar plates, developed at Los Alamos National Laboratory, is made of a blend of compounds (i.e., porous graphite, polycarbonate, and stainless steel). This mixture allows a reduction of the cost associated with graphite processing, since treating a more porous material is less expensive. The waterproofing characteristic is provided by plastic polycarbonate and steel; the latter also yields rigidity and mechanical strength to the whole structure. On the other hand, polycarbonate creates a barrier against chemical attacks and also features high shapeability. In recent years, these types of multi-material plates have become increasingly popular as an alternative that combines mechanical and chemical stability with reduced costs [115].

Two of the main car manufacturers, Honda, and Toyota, include metal bipolar plates in the fuel-cell stacks installed in their models. However, processing metal plates bears significantly higher costs than other materials, as the material, 316 L coated stainless steel, is typically selected. However, the use of metal bipolar plates is affected by two negative aspects [113]. As previously mentioned, the first concerns corrosion that occurs at the anode, where the released metal ions can bond with the protons of the ionomer in the

electrode and the membrane, thus causing an increase in the resistance of the electrode and of the membrane. The second problem occurs at the cathode, where an increase in contact resistance caused by the accumulation of an oxide layer may arise, with the latter showing lower conductivity than the metal itself. Many studies have been conducted to address those drawbacks, such as thermal nitration on metal alloys (based on Ni and Fe), coating of nitride plates (e.g., Cr, Ti, TiAl, Al) [116,117], or deposition of an Au film that meets the requirements in terms of oxidation stability and electrical conduction. Unfortunately, the last strategy is not conducive to cost reduction. As an order of magnitude, the cost of bipolar plates impacts on the total cost of fuel-cell stacks by 25–40%, with its value ranging from 25 to 50 USD/kW [81]. This relatively wide span depends mostly on the ability to create an economy of scale and on the materials involved.

Flow channels of bipolar plates are aimed at both removing the formed amount of water and at distributing the reagents uniformly towards the MEA; they are actually hosted on the surface of the bipolar plates. The areas between channels, in the space between two adjacent cells of the same stack, are used to collect and transport electric current and heat generated in the MEA. If water remains in the channels and is not made to flow away, there are not only problems with transferring the reacting gases, but also pressure drops that make current distribution inhomogeneous over the aforementioned areas, thus implying a consequent reduction in performance. To address these problems, channel geometry can be adapted and varied: among the possible design strategies, parallel, interdigitated, and serpentine channels are the most popular [118].

Gaskets of bipolar plates are also particularly important to achieve a virtually full prevention against the escape of the reactants to the outside through the whole thickness of the cell, thus compensating for the inherent variability in thickness of the various other components. Usually, a special rubber is selected, exhibiting mechanical and thermal resistance characteristics, flexibility and chemically stability within a reducing, oxidizing and acid environment. The most common materials used are ethylene-propylene-diene-monomer (EPDM), butyl rubber (IRR), or fluorinated rubbers (FKM, such as Viton®). The cost of gaskets is often included in that of bipolar plates or MEA when assessing the relative impact of the components on the total cost of the fuel-cell stacks used in the automotive sector.

4.6. Thermal and Water Management

In conventional cars propelled by ICE, heat generation takes place mostly in the engine body, and heat is largely carried away by the exhaust gases. On the other hand, in fuel cells heat is generally kept within, so over 95% of it shall be managed by a dedicated system for external cooling. With quite an expected outcome, this is one of the most significant subsystems governing the performance of the entire fuel-cell stack [119], also because poor thermal management would lead to an internal heat imbalance within the MEA and specifically in the polymeric membrane. This latter is particularly sensitive to the presence of water, as remarked in Section 4.1. The rapid variation in heat generation is associated with actual driving cycles, which can cause additional thermal and mechanical stress that can damage the materials involved and consequently the whole stack [120]. Into this context, the main cooling methods used for this purpose are liquid cooling, air cooling, and phase change materials [121–125].

Water management is the control, not only of water in its liquid phase, but also of the vapor phase. Transport of liquid water in the flow channels and optimization of water discharge are instrumental in achieving high performance, thus requiring dedicated design [126–132]. Notably, the production of water vapor from electrochemical reactions leads to its condensation; water as a liquid can flood the pores of the electrodes, which is indeed the well-known water flooding phenomenon. In such conditions, water acts as a plug that reduces the feeding speed of the reagents to the reaction sites, thus becoming detrimental to the performance of each cell and therefore of the entire stack. The presence

of water and an unsuitable distribution of it within the channels may also cause corrosion of carbon compounds included within of the bipolar plates.

It is worth noting that the auxiliary systems inserted in the FCEV to perform thermal and water management of the fuel-cell stack are often included within the balance of plant (BoP), together with several other components used to supply and circulate the required reactants. Liquid cooling—usually by deionized water—is typical of applications where power is of 100-kW order of magnitude; that subsystem features a hydraulic circuit with a radiator and a pump; an intercooler is often added to exploit the temperature difference between hot water (i.e., the coolant) downstream of the stack and air at the inlet. Water management may require a humidifier for the incoming air, to be inserted upstream of the stack inlet; however, humidification of PEMFC membranes is usually performed by water crossover from cathode to anode. A water recovery system is also often provided. As an estimate, the cooling subsystem embodies a share of about 15% of the total BoP cost, while the most impactful components are the air compressor, the share of which is slightly lower than 50%, and the balance of system (e.g., sensors and controllers), amounting to about 25% [81]. In FCEV, the cost of the fuel-cell system is made by two main entries: stack (about 75%) and BoP (about 25%) costs. For instance, the overall cost of the Toyota Mirai fuel-cell system is about 235 USD/kW, with 170 USD/kW associated to the stack and 65 USD/kW to the BoP [124].

5. Conclusions and Future Directions

In line with the objectives of the European Green Deal, in July 2020, the European Commission (EC) also identified a strategy to create the conditions for a massive diffusion of hydrogen within Europe in the coming years. The scope comprises the automotive sector, which in fact would serve as the magnet for hydrogen economy. To make hydrogen propulsion viable, it is necessary to match supply and demand, firstly by solving the infrastructural problems associated with the distribution network and the availability of refueling stations. From that standpoint, Europe is making steps forward, both by urging the construction of hubs aimed at beginning a fast-growing infrastructural expansion, and by supporting the construction of electrolyzers, to produce up to 10 million tons of hydrogen in Europe by 2030. These aspects will govern the hydrogen cost in the near- to medium-term horizon, which is a significant parameter in the calculation of the total cost of ownership (TCO). As already mentioned, the comparison between FCEV—with FCHEV included—and BEV, with a focus on the viability of fuel cells, a parameter of extreme importance, is also the cost per unit power. Those figures also highlight the impactful effect of production volumes: fuel-cell cost per unit power could be brought down to about USD 80/kW in 2030, if fuel-cell production reached 100,000 pieces per year. Generally, it appears crucial for manufacturers both to continue reducing costs of their fuel-cell models and to create partnerships that aim at increasing the volumes on the market by integrating the same fuel-cell stacks in different cars. As reported and described in detail within Section 4, research on new materials may be particularly instrumental in achieving a substantial cost reduction. Accomplishing this quest appears feasible in a short- to medium-term horizon with regard to the fuel-cell membrane and bipolar plates. However, discovering or developing new (and nonprecious) catalysts capable of matching the action currently realized by platinum is still a major challenge, even though promising results have been brought in the recent literature on this specific aspect.

To evaluate the degree of acceptance of fuel-cell technology, it is necessary to progress with the analysis of TCO and in particular with the economic comparison between the fuel-cell-based powertrain and the battery-powered one; that includes electric motors, batteries, fuel cells, storage, power electronics and control systems. Furthermore, it is necessary to evaluate the variable costs associated with the energy sources (i.e., electricity for BEV and hydrogen for fuel cells), the variable costs linked to maintenance operations (ordinary and extraordinary), and taxes. In addition to these elements, the manufacturer's markup may also be considered since it typically covers development costs and profit.

Therefore, making fuel cells penetrate the automotive market may imply a continuous growth over some years in the future. For this same reason, hydrogen-fueled ICE may be considered an excellent solution to satisfy an immediate request for eliminating carbon emissions in a short timeframe, while waiting for fuel-cell costs to decrease by the onset of a dedicated economy of scale.

Finally, all aspects of safety in hydrogen storage and distribution will likely pose as the main challenges as popularity of hydrogen and fuel cells grows. There have been and currently are numerous research efforts spent on these challenges, with the application of new European regulations being a step forward in terms of awareness of the inherent problems related to managing hydrogen. Safety requirements are usually complied with by enforcing the stringent resistance requirements of the tanks, by ensuring the presence of pressure regulating and limiting valves, and by continuous monitoring of hydrogen concentration in all the compartments of a vehicle through sensors capable of detecting leakages. It is worth noting that the design of fuel-cell cars mostly follows the regulatory standards (e.g., the UN R134 standard) that rule any hydrogen-powered vehicles.

References

1. Bailey, D. *How the Automobile Changed History*; ABDO: North Mankato, MN, USA, 2016.
2. Muratori, M.; Marano, V.; Rizzo, G.; Rizzoni, G. Electric mobility: From fossil fuels to renewable energy, opportunities and challenges. *IFAC Proc. Vol.* **2013**, *46*, 812–817.
3. Andersen, L.G.; Larsen, J.K.; Fraser, E.S.; Schmidt, B.; Dyre, J.C. Rolling resistance measurement and model development. *J. Transp. Eng.* **2015**, *141*, 04014075.
4. Babin, T.; Sangeetha, N.; Sudalaiyandi, D.P. Reducing the drag resistance of automotive cars by diminishing the wake separation zone. *AIP Conf. Proc.* **2018**, *2039*, 020078.
5. Zhang, D.; Ivanco, A.; Filipi, Z. Model-based estimation of vehicle aerodynamic drag and rolling resistance. *SAE Int. J. Commer. Veh.* **2015**, *8*, 433–439.
6. Andwari, A.M.; Pesiridis, A.; Rajoo, S.; Martinez-Botas, R.; Esfahanian, V. A review of Battery Electric Vehicle technology and readiness levels. *Renew. Sustain. Energy Rev.* **2017**, *78*, 414–430.
7. Offer, G.J.; Howey, D.; Contestabile, M.; Clague, R.; Brandon, N.P. Comparative analysis of battery electric, hydrogen fuel cell and hybrid vehicles in a future sustainable road transport system. *Energy Policy* **2010**, *38*, 24–29.
8. Ozsoysal, O.A. Effects of combustion efficiency on an Otto cycle. *Int. J. Exergy* **2010**, *7*, 232–242. [CrossRef]
9. Gupta, H.N. *Fundamentals of Internal Combustion Engines*; PHI Learning: Delhi, India, 2009.
10. Villante, C.; Genovese, A. Hydromethane: A bridge towards the hydrogen economy or an unsustainable promise? *Int. J. Hydrogen Energy* **2012**, *37*, 11541–11548.
11. Stan, C. *Alternative Propulsion for Automobiles*; Springer: Cham, Switzerland, 2017.
12. Jain, P.C. Climate change, greenhouse effect and climate change: Scientific basis and overview. *Renew. Energy* **1993**, *4–5*, 403–420.
13. United States Environmental Protection Agency (EPA). EPA's Report on the Environment (ROE). Available online: https://www.epa.gov/report-environment (accessed on 14 February 2023).
14. United States Environmental Protection Agency (EPA). *Air Toxics from Motor Vehicles*; Fact sheet EPA 400-F-92-004; United States Environmental Protection Agency: Washington, DC, USA, 1995.
15. Onofri, M.; Bernabeo, R.A.; Webster, K. Health and environmental impacts of NOx: An ultra-low level of NOx (oxides of nitrogen) achievable with a new technology. *Glob. J. Eng. Sci.* **2019**, *2*, GJES.MS.ID.000540.
16. Kurt, O.K.; Zhang, J.; Pinkerton, K.E. Pulmonary health effects of air pollution. *Curr. Opin. Pulm. Med.* **2016**, *22*, 138–143. [CrossRef]
17. Orellano, P.; Reynoso, J.; Quaranta, N. Short-term exposure to sulphur dioxide (SO_2) and all-cause and respiratory mortality: A systematic review and meta-analysis. *Environ. Int.* **2021**, *150*, 106434. [CrossRef]
18. Stone, R.; Ball, J.K. *Automotive Engineering Fundamentals*; SAE International: Warrendale, PA, USA, 2004.

19. Zhang, H.; Sun, C.; Ge, M. Review of the research status of cost-effective zinc–iron redox flow batteries. *Batteries* **2022**, *8*, 202. [CrossRef]

20. Abdin, A.; Zafaranloo, A.; Rafiee, A.; Mérida, W.; Lipiński, W.; Khalilpour, K.L. Hydrogen as an energy vector. *Renew. Sustain. Energy Rev.* **2020**, *120*, 109620. [CrossRef]

21. Buekers, J.; Van Holderbeke, M.; Bierkens, J.; Int Panis, L. Health and environmental benefits related to electric vehicle introduction in EU countries. *Transp. Res. D Transp. Environ.* **2014**, *33*, 26–38. [CrossRef]

22. Hermesmann, M.; Müller, T.E. Green, turquoise, blue, or grey? Environmentally friendly hydrogen production in transforming energy systems. *Prog. Energy Combust. Sci.* **2022**, *90*, 100996. [CrossRef]

23. Megía, P.J.; Vizcaíno, A.J.; Calles, J.A.; Carrero, A. Hydrogen production technologies: From fossil fuels toward renewable sources. A mini review. *Energy Fuels* **2021**, *35*, 16403–16415. [CrossRef]

24. Espegren, K.; Damman, S.; Pisciella, P.; Graabak, I.; Tomasgar, A. The role of hydrogen in the transition from a petroleum economy to a low-carbon society. *Int. J. Hydrogen Energy* **2021**, *46*, 23125–23138. [CrossRef]

25. Taipabu, M.I.; Viswanathan, K.; Wu, W.; Hattu, N.; Atabani, A.E. A critical review of the hydrogen production from biomass-based feedstocks: Challenge, solution, and future prospect. *Process Saf. Environ. Prot.* **2022**, *164*, 384–407. [CrossRef]

26. García, L. Hydrogen production by steam reforming of natural gas and other nonrenewable feedstocks. In *Compendium of Hydrogen Energy—Hydrogen Production and Purification*; Subramani, V., Basile, A., Nejat Veziroğlu, T., Eds.; Woodhead Publishing: Sawston, UK, 2015; Chapter 4, pp. 83–107.

27. Sengodan, S.; Lan, R.; Humphreys, J.; Du, D.; Xu, W.; Wang, H.; Tao, S. Advances in reforming and partial oxidation of hydrocarbons for hydrogen production and fuel cell applications. *Renew. Sustain. Energy Rev.* **2018**, *82*, 761–780. [CrossRef]

28. Agyekum, E.B.; Nutakor, C.; Agwa, A.M.; Kamel, S. A critical review of renewable hydrogen production methods: Factors affecting their scale-up and its role in future energy generation. *Membranes* **2022**, *12*, 173. [CrossRef]

29. Shiva Kumar, S.; Himabindu, V. Hydrogen production by PEM water electrolysis—A review. *Mater. Sci. Energy Technol.* **2019**, *2*, 442–454. [CrossRef]

30. Kalinci, Y.; Hepbasli, A.; Dincer, I. Biomass-based hydrogen production: A review and analysis. *Int. J. Hydrogen Energy* **2009**, *34*, 8799–8817. [CrossRef]

31. Yalçin, S. A review of nuclear hydrogen production. *Int. J. Hydrogen Energy* **1989**, *14*, 551–561. [CrossRef]

32. Ishaq, H.; Dincer, I.; Crawford, C. A review on hydrogen production and utilization: Challenges and opportunities. *Int. J. Hydrogen Energy* **2022**, *47*, 26238–26264. [CrossRef]

33. Lee, J.E.; Shafiq, I.; Hussain, M.; Lam, S.S.; Rhee, G.H.; Park, Y.K. A review on integrated thermochemical hydrogen production from water. *Int. J. Hydrogen Energy* **2022**, *47*, 4346–4356. [CrossRef]

34. Das, D.; Nejat Veziroğlu, T. Hydrogen production by biological processes: A survey of literature. *Int. J. Hydrogen Energy* **2001**, *26*, 13–28. [CrossRef]

35. Lopez, G.; Santamaria, L.; Lemonidou, A.; Zhang, S.; Wu, C.; Sipra, A.T.; Gao, N. Hydrogen generation from biomass by pyrolysis. *Nat. Rev. Methods Prim.* **2022**, *2*, 20. [CrossRef]

36. Parthasarathy, P.; Sheeba Narayanan, K. Hydrogen production from steam gasification of biomass: Influence of process parameters on hydrogen yield—A review. *Renew. Energy* **2014**, *66*, 570–579. [CrossRef]

37. Forruque Ahmed, S.; Rafa, N.; Mofijur, M.; Anjum Badruddin, I.; Inayat, A.; Sawkat Ali, M.; Farrok, O.; Yunus Khan, T.M. Biohydrogen production from biomass sources: Metabolic pathways and economic analysis. *Front. Energy Res.* **2021**, *9*, 753878. [CrossRef]

38. Amirthan, T.; Perera, M.S.A. The role of storage systems in hydrogen economy: A review. *J. Nat. Gas Sci. Eng.* **2022**, *108*, 104843. [CrossRef]

39. US DRIVE Partnership. *Target Explanation Document: Onboard Hydrogen Storage for Light-Duty Fuel Cell Vehicles*; US Department of Energy: Washington, DC, USA, 2017.

40. Satyapal, S.; Petrovic, J.; Read, C.; Thomas, G.; Ordaz, G. The U.S. Department of Energy's National Hydrogen Storage Project: Progress towards meeting hydrogen-powered vehicle requirements. *Catal. Today* **2007**, *120*, 246–256. [CrossRef]

41. Nash, D.; Aklil, D.; Johnson, E.; Gazey, R.; Ortisi, V. Hydrogen storage: Compressed gas. In *Comprehensive Renewable Energy*; Sayigh, A., Ed.; Elsevier: Amsterdam, The Netherlands, 2012; Chapter 4.05, pp. 131–155.

42. Chen, Y.; Zhao, S.; Ma, H.; Wang, H.; Hua, L.; Fu, S. Analysis of hydrogen embrittlement on aluminum alloys for vehicle-mounted hydrogen storage tanks: A review. *Metals* **2021**, *11*, 1303. [CrossRef]

43. Alves, M.P.; Gul, W.; Cimini Junior, C.A.; Ha, S.K. A review on industrial perspectives and challenges on material, manufacturing, design and development of compressed hydrogen storage tanks for the transportation sector. *Energies* **2022**, *15*, 5152. [CrossRef]

44. Nejat Veziroglu, T.; Barbir, F. Hydrogen: The wonder fuel. *Int. J. Hydrogen Energy* **1992**, *17*, 391–404. [CrossRef]

45. Rico-Zavala, A.; Gurrola, M.P.; Arriaga, L.G.; Banuelos, J.A.; Álvarez-Contreras, L.; Carbone, A.; Saccà, A.; Matera, F.V.; Pedicini, R.; Álvarez, A.; et al. Synthesis and characterization of composite membranes modified with Halloysite nanotubes and phosphotungstic acid for electrochemical hydrogen pumps. *Renew. Energy* **2018**, *122*, 163–172. [CrossRef]

46. Aziz, M. Liquid hydrogen: A review on liquefaction, storage, transportation, and safety. *Energies* **2021**, *14*, 5917. [CrossRef]

47. Pedicini, R.; Gatto, I.; Gatto, M.F.; Passalacqua, E. Carbonaceous materials in hydrogen storage. In *Hydrogen Storage Technologies*; Sankir, M., Demirci Sankir, N., Eds.; Wiley: Hoboken, NJ, USA, 2018; Chapter 7, pp. 260–298.

48. Chen, P.; Akiba, E.; Orimo, S.; Zuettel, A.; Schlapbach, L. Hydrogen storage by reversible metal hydride formation. In *Hydrogen Science and Engineering: Materials, Processes, Systems and Technology*; Stolten, D., Emonts, B., Eds.; Wiley: Hoboken, NJ, USA, 2016; Chapter 31, pp. 763–790.

49. Pedicini, R.; Gatto, I.; Passalacqua, E. Solid-state materials for hydrogen storage. In *Nanostructured Materials for Next-Generation Energy Storage and Conversion*; Li, F., Bashir, S., Liu, J.L., Eds.; Springer: Heidelberg, Germany, 2018; Volume 2, Chapter 15, pp. 443–467.

50. Friedlmeier, G.; Groll, M. Experimental analysis and modeling of the hydriding kinetics of Ni-doped and pure Mg. *J. Alloys Compd.* **1997**, *253–254*, 550–555. [CrossRef]

51. Kumar, S.; Miyaoka, H.; Ichikawa, T.; Dey, G.K.; Kojima, Y. Micro-alloyed Mg_2Ni for better performance as negative electrode of Ni-MH battery and hydrogen storage. *Int. J. Hydrogen Energy* **2017**, *42*, 5220–5226. [CrossRef]

52. Yang, J.; Sudik, A.; Wolverton, C.; Siegel, D.J. High capacity hydrogen storage materials: Attributes for automotive applications and techniques for materials discovery. *Chem. Soc. Rev.* **2010**, *39*, 656–675. [CrossRef]

53. Liu, Y.; Yang, Y.; Zhou, Y.; Zhang, Y.; Gao, M.; Pan, H. Hydrogen storage properties and mechanisms of the $Mg(BH_4)_2$–$NaAlH_4$ system. *Int. J. Hydrogen Energy* **2012**, *37*, 17137–17145. [CrossRef]

54. Zittel, W.; Wurster, R. *Hydrogen in the Energy Sector*; Ludwig-Bölkow-Systemtechnik: Ottobrunn, Germany, 1996.

55. Taylor, J.B.; Alderson, J.E.A.; Kalyanam, K.M.; Lyle, A.B.; Phillips, L.A. A technical and economic assessment of methods for the storage of large quantities of hydrogen. *Int. J. Hydrogen Energy* **1986**, *11*, 5–22. [CrossRef]

56. Peters, M.S.; Timmerhaus, K.D.; West, R.E. *Plant Design and Economics for Chemical Engineers*; McGraw-Hill: New York City, NY, USA, 2003.

57. Fan, L.; Tu, Z.; Chan, S.H. Recent development of hydrogen and fuel cell technologies: A review. *Energy Rep.* **2021**, *7*, 8421–8446. [CrossRef]

58. Marin, G.D.; Naterer, G.F.; Gabriel, K. Rail transportation by hydrogen vs. electrification—Case study for Ontario, Canada, II: Energy supply and distribution. *Int. J. Hydrogen Energy* **2010**, *35*, 6097–6107. [CrossRef]

59. Alkhaledi, A.N.F.N.R.; Sampath, S.; Pilidis, P. A hydrogen fuelled LH2 tanker ship design. *Ships Offshore Struct.* **2022**, *17*, 1555–1564. [CrossRef]

60. Jankiewicz, S.P.; Siang, C.C.; Yao, X.; Santangelo, P.E.; Marshall, A.W.; Roby, R.J. Analyzing fire-induced dispersion and detector response in complex enclosures using salt-water modeling. *Fire Saf. J.* **2014**, *65*, 19–29. [CrossRef]

61. Santangelo, P.E.; Jacobs, B.C.; Ren, N.; Sheffel, J.A.; Corn, M.L.; Marshall, A.W. Suppression effectiveness of water-mist sprays on accelerated wood-crib fires. *Fire Saf. J.* **2014**, *70*, 98–111. [CrossRef]

62. Santangelo, P.E.; Tarozzi, L.; Tartarini, P. Full-scale experiments of fire control and suppression in enclosed car parks: A comparison between sprinkler and water-mist systems. *Fire Technol.* **2016**, *52*, 1369–1407. [CrossRef]

63. Santangelo, P.E.; Tarozzi, L.; Tartarini, P. Full-scale experiments of water-mist systems for control and suppression of sauna fires. *Fire* **2022**, *5*, 214. [CrossRef]

64. Li, H.; Niu, R.; Li, W.; Lu, H.; Cairney, J.; Chen, Y.S. Hydrogen in pipeline steels: Recent advances in characterization and embrittlement mitigation. *J. Nat. Gas Sci. Eng.* **2022**, *105*, 104709. [CrossRef]

65. Strianese, M.; Torricelli, N.; Tarozzi, L.; Santangelo, P.E. Experimental assessment of the acoustic performance of nozzles designed for clean agent fire suppression. *Appl. Sci.* **2023**, *13*, 186. [CrossRef]

66. Yee, R.S.L.; Rozendal, R.A.; Zhang, K.; Ladewig, B.P. Cost effective cation exchange membranes: A review. *Chem. Eng. Res. Des.* **2012**, *90*, 950–959. [CrossRef]

67. Watanabe, M. Structure of Electrochemical Cell for Wetting Diaphragm of Solid Polymer Electrolyte. European Patent EP0499593A1, 2 May 2001.

68. Vanderborgh, N.E.; Hadstrom, J.C. Fuel Cell Water Transport. US Patent US4973530A, 27 November 1990.

69. Laribi, S.; Mammar, K.; Sahli, Y.; Koussa, K. Air supply temperature impact on the PEMFC impedance. *J. Energy Storage* **2018**, *17*, 327–335. [CrossRef]

70. Murugesan, K.; Senniappan, V. Investigation of water management dynamics on the performance of a Ballard-Mark-V Proton Exchange Membrane Fuel Cell stack system. *Int. J. Electrochem. Sci.* **2013**, *8*, 7885–7904.

71. Wehkamp, N.; Breitwieser, M.; Büchler, A.; Klingele, B.M.; Zengerle, R.; Thiele, S. Directly deposited Nafion/TiO2 composite membranes for high power medium temperature fuel cells. *RSC Adv.* **2016**, *6*, 24261–24266. [CrossRef]

72. Chien, H.C.; Tsai, L.D.; Lai, C.M.; Lin, J.N.; Zhu, C.Y.; Chang, F.C. Characteristics of high-water-uptake activated carbon/Nafion hybrid membranes for proton exchange membrane fuel cells. *J. Power Sources* **2013**, *226*, 87–93. [CrossRef]

73. Peron, J.; Mani, A.; Zhao, X.; Edwards, D.; Adachi, M.; Soboleva, T.; Shi, Z.; Xie, Z.; Navessin, T.; Holdcroft, S. Properties of Nafion® NR-211 membranes for PEMFCs. *J. Membr. Sci.* **2010**, *356*, 44–51.

74. Shi, S.; Chen, G.; Wang, Z.; Chen, X. Mechanical properties of Nafion 212 proton exchange membrane subjected to hygrothermal aging. *J. Power Sources* **2013**, *238*, 318–323. [CrossRef]

75. Kúš, P. *Thin-Film Catalysts for Proton Exchange Membrane Water Electrolyzers and Unitized Regenerative Fuel Cells*; Springer: Cham, Switzerland, 2019.

76. Jeon, Y.; Hwang, H.; Park, J.; Hwang, H.; Shul, Y.G. Temperature-dependent performance of the polymer electrolyte membrane fuel cell using short-side-chain perfluorosulfonic acid ionomer. *Int. J. Hydrogen Energy* **2014**, *39*, 11690–11699. [CrossRef]

77. Lin, H.L.; Yu, T.L.; Han, F.H. A method for improving ionic conductivity of Nafion membranes and its application to PEMFC. *J. Polym. Res.* **2006**, *13*, 379–385.

78. Yu, T.L.; Lin, H.L.; Shen, K.S.; Huang, L.N.; Chang, Y.C.; Jung, G.B.; Huang, J.C. Nafion/PTFE composite membranes for fuel cell applications. *J. Polym. Res.* **2004**, *11*, 217–224. [CrossRef]

79. Sone, Y.; Ekdunge, P.; Simonsson, D. Proton conductivity of Nafion 117 as measured by a four-electrode AC impedance method. *J. Electrochem. Soc.* **1996**, *143*, 1254–1259. [CrossRef]

80. Bose, S.; Kuila, T.; Nguyen, T.X.H.; Kim, N.H.; Lau, K.; Lee, J.H. Polymer membranes for high temperature proton exchange membrane fuel cell: Recent advances and challenge. *Prog. Polym. Sci.* **2011**, *36*, 813–843. [CrossRef]

81. James, B.D.; Huya-Kouadio, J.M.; Houcins, C.; DeSantis, D.A. *Mass Production Cost Estimation of Direct H₂ PEM Fuel Cell Systems for Transportation Applications: 2016 Update*; Strategic Analysis: Arlington, VA, USA, 2016.

82. Sun, X.; Simonsen, S.C.; Norby, T.; Chatzitakis, A. Composite membranes for High Temperature PEM Fuel Cells and electrolysers: A critical review. *Membranes* **2019**, *9*, 83. [CrossRef] [PubMed]

83. Saccà, A.; Carbone, A.; Gatto, I.; Pedicini, R.; Passalacqua, E. Synthesized Yttria Stabilised Zirconia as filler in Proton Exchange Membranes (PEMs) with enhanced stability. *Polym. Test.* **2018**, *65*, 322–330. [CrossRef]

84. Sun, C.; Negro, E.; Nale, A.; Pagot, G.; Vezzù, K.; Zawodzinski, T.A.; Meda, L.; Gambaro, C.; Di Noto, V. An efficient barrier toward vanadium crossover in redox flow batteries: The bilayer [Nafion/(WO₃)ₓ] hybrid inorganic-organic membrane. *Electrochim. Acta* **2021**, *378*, 138133. [CrossRef]

85. Carbone, A.; Gaeta, M.; Romeo, A.; Portale, G.; Pedicini, R.; Gatto, I.; Castriciano, M.A. Porphyrin/sPEEK membranes with improved conductivity and durability for PEFC technology. *ACS Appl. Energy Mater.* **2018**, *1*, 1664–1673. [CrossRef]

86. Carbone, A.; Pedicini, R.; Gatto, I.; Saccà, A.; Patti, A.; Bella, G.; Cordaro, M. Development of polymeric membranes based on quaternized polysulfones for AMFC applications. *Polymers* **2020**, *12*, 283. [CrossRef]

87. Rajabi, Z.; Javanbakht, M.; Hooshyari, K.; Adibi, M.; Badiei, A. Phosphoric acid doped polybenzimidazole based polymer electrolyte membrane and functionalized SBA-15 mesoporous for elevated temperature fuel cell. *Int. J. Hydrogen Energy* **2021**, *46*, 33241–33259. [CrossRef]

88. Atanasoski, R.; Dodelet, J.-P. Fuel cells—Proton-Exchange Membrane Fuel Cells Catalysts: Non-platinum. In *Encyclopedia of Electrochemical Power Sources*; Garche, J., Ed.; Elsevier: Amsterdam, The Netherlands, 2009; pp. 639–649.

89. Gatto, I.; Saccà, A.; Carbone, A.; Pedicini, R.; Passalacqua, E. MEAs for Polymer Electrolyte Fuel Cell (PEFC) working at medium temperature. *J. Fuel Cell Sci. Technol.* **2006**, *3*, 361–365. [CrossRef]

90. Tasic, G.S.; Miljanic, S.S.; Kaninski, M.P.M.; Saponjic, D.P.; Nikolic, V.M. Non-noble metal catalyst for a future Pt free PEMFC. *Electrochem. Commun.* **2009**, *11*, 2097–2100. [CrossRef]

91. Wang, B. Recent development of non-platinum catalysts for oxygen reduction reaction. *J. Power Sources* **2005**, *152*, 1–15. [CrossRef]

92. Harrison, K.W.; Martin, G.D.; Ramsden, T.G. *The Wind-to-Hydrogen Project: Operational Experience, Performance Testing, and Systems Integration*; Technical report NREL/TP-550-44082; National Renewable Energy Laboratory: Golden, CO, USA, 2009.

93. Chong, L.; Wen, J.; Kubal, J.; Sen, F.G.; Zou, J.; Greeley, J.; Chan, M.; Barkholtz, H.; Ding, W.; Liu, D.-J. Ultralow-loading platinum-cobalt fuel cell catalysts derived from imidazolate frameworks. *Science* **2018**, *362*, 1276–1281. [CrossRef] [PubMed]

94. Wang, C.; An, C.; Qin, C.; Gomaa, H.; Deng, Q.; Wu, S.; Hu, N. Noble metal-based catalysts with core-shell structure for oxygen reduction reaction: Progress and prospective. *Nanomaterials* **2022**, *12*, 2480. [CrossRef] [PubMed]

95. Mu, Y.-T.; Weber, A.Z.; Gu, Z.-L.; Tao, W.-Q. Mesoscopic modeling of transport resistances in a polymer-electrolyte fuel-cell catalyst layer: Analysis of hydrogen limiting currents. *Appl. Energy* **2019**, *255*, 113895. [CrossRef]

96. Ganesan, R.; Lee, J.S. Tungsten carbide microspheres as a noble-metal-economic electrocatalyst for methanol oxidation. *Angew. Chem. Int. Ed.* **2005**, *44*, 6557–6560. [CrossRef]

97. Barnett, C.J.; Burstein, G.T.; Kucernak, A.R.; Williams, K.R. Electrocatalytic activity of some carburised nickel, tungsten and molybdenum compounds. *Electrochim. Acta* **1997**, *42*, 2381–2388. [CrossRef]

98. Shi, Z.; Zhang, J. Density functional theory study of transitional metal macrocyclic complexes' dioxygen-binding abilities and their catalytic activities toward oxygen reduction reaction. *J. Phys. Chem. C* **2007**, *111*, 7084–7090. [CrossRef]

99. Iyuke, S.E.; Mohamad, A.B.; Kadhum, A.A.H.; Daud, W.R.W.; Rachid, C. Improved membrane and electrode assemblies for proton exchange membrane fuel cells. *J. Power Sources* **2003**, *114*, 195–202. [CrossRef]

100. Dao, D.V.; Adilbish, G.; Lee, I.H.; Yu, Y.T. Enhanced electrocatalytic property of Pt/C electrode with double catalyst layers for PEMFC. *Int. J. Hydrogen Energy* **2019**, *44*, 24580–24590.

101. Cannio, M.; Righi, S.; Santangelo, P.E.; Romagnoli, M.; Pedicini, R.; Carbone, A.; Gatto, I. Smart catalyst deposition by 3D printing for Polymer Electrolyte Membrane Fuel Cell manufacturing. *Renew. Energy* **2021**, *163*, 414–422. [CrossRef]

102. Gould, B.D.; Rodgers, J.A.; Schuette, M.; Bethune, K.; Louis, S.; Rocheleau, R.; Swyder-Lyons, K. Performance and limitations of 3D-printed bipolar plates in fuel cells. *ECS J. Solid State Sci. Technol.* **2015**, *4*, P3063. [CrossRef]

103. Huang, W.; Finnerty, C.; Sharp, R.; Wang, K.; Balili, B. High-performance 3D printed microtubular Solid Oxide Fuel Cells. *Adv. Mater. Technol.* **2017**, *2*, 1600258. [CrossRef]

104. Wang, X.; Ma, H.; Peng, H.; Wang, Y.; Wang, G.; Xiao, L.; Lu, J.; Zhuang, L. Enhanced mass transport and water management of polymer electrolyte fuel cells via 3-D printed architectures. *J. Power Sources* **2021**, *515*, 230636. [CrossRef]

105. Piri, H.; Bi, X.T.; Li, H.; Wang, H. 3D-printed fuel-cell bipolar plates for evaluating flow-field performance. *Clean Energy* **2020**, *4*, 142–157. [CrossRef]

106. Pelaccia, R.; Santangelo, P.E. A Homogeneous Flow Model for nitrogen cooling in the aluminum-alloy extrusion process. *Int. J. Heat Mass Transf.* **2022**, *195*, 123202. [CrossRef]

107. GASKATEL Gas Diffusion Electrodes. Available online: https://gaskatel.de/en/gas-diffusion-electrodes/ (accessed on 15 February 2023).

108. Millington, B.; Whipple, V.; Pollet, B.G. A novel method for preparing proton exchange membrane fuel cell electrodes by the ultrasonic-spray technique. *J. Power Sources* **2011**, *196*, 8500–8508. [CrossRef]

109. Santangelo, P.E.; Allesina, G.; Bolelli, G.; Lusvarghi, L.; Matikainen, V.; Vuoristo, P. Infrared thermography as a Non-Destructive Testing solution for thermal spray metal coatings. *J. Therm. Spray Technol.* **2017**, *26*, 1982–1993. [CrossRef]

110. Santangelo, P.E.; Romagnoli, M.; Puglia, M. An experimental approach to evaluate drying kinetics and foam formation in inks for inkjet printing of fuel-cell layers. *Exp. Therm. Fluid Sci.* **2022**, *135*, 110631. [CrossRef]

111. Willert, A.; Tabary, F.Z.; Zubkova, T.; Santangelo, P.E.; Romagnoli, M.; Baumann, R.R. Multilayer additive manufacturing of catalyst-coated membranes for polymer electrolyte membrane fuel cells by inkjet printing. *Int. J. Hydrogen Energy* **2022**, *47*, 20973–20986. [CrossRef]

112. Heinzel, A.; Mahlendorf, F.; Niemzig, O.; Kreuz, C. Injection moulded low-cost bipolar plates for PEM fuel cells. *J. Power Sources* **2004**, *131*, 35–40. [CrossRef]

113. de Bruijn, F.A.; Makkus, R.C.; Mallant, R.K.A.M.; Janssen, G.J.M. Materials for state-of-the-art PEM fuel cells, and their suitability for operation above 100 °C. In *Advances in Fuel Cells*; Elsevier: Amsterdam, The Netherlands, 2007; Volume 1, Chapter 5, pp. 235–336.

114. Włodarczyk, R.K. Porous composite for bipolar plate in low emission hydrogen fuel cells. *J. Ecol. Eng.* **2018**, *19*, 225–232. [CrossRef]

115. Busick, D.N.; Wilson, M.S. *Low-Cost Composite Materials for PEFC Bipolar Plates*; Report LA-UR-R-98-4129; Los Alamos National Laboratory: Los Alamos, NM, USA, 1999.

116. Cho, E.A.; Jeon, U.S.; Hong, S.A.; Oh, I.H.; Kang, S.G. Performance of a 1-kW-class PEMFC stack using TiN-coated 316 stainless steel bipolar plates. *J. Power Sources* **2005**, *142*, 177–183. [CrossRef]

117. Mepsted, G.O.; Moore, J.M. Performance and durability of bipolar plate materials. In *Handbook of Fuel Cells*; Wiley: Hoboken, NJ, USA, 2010.

118. Kahraman, H.; Orhan, M.F. Flow field bipolar plates in a proton exchange membrane fuel cell: Analysis & modeling. *Energy Convers. Manag.* **2017**, *133*, 363–384.

119. Baroutaji, A.; Arjunan, A.; Ramadan, M.; Robinson, J.; Alaswad, A.; Abdelkareem, M.A.; Olabi, A.G. Advancements and prospects of thermal management and waste heat recovery of PEMFC. *Int. J. Thermofluids* **2021**, *9*, 100064. [CrossRef]

120. İnci, M.; Buyuk, M.; Demir, M.H.; Ilbey, G. A review and research on fuel cell electric vehicles: Topologies, power electronic converters, energy management methods, technical challenges, marketing and future aspects. *Renew. Sustain. Energy Rev.* **2021**, *137*, 110648. [CrossRef]

121. Ramos-Alavarado, B.; Li, P.; Liu, H.; Hernandez-Guerrero, A. CFD study of liquid-cooled heat sinks with microchannel flow field configurations for electronics, fuel cells, and concentrated solar cells. *Appl. Therm. Eng.* **2011**, *31*, 2494–2507. [CrossRef]

122. Santangelo, P.E.; Corticelli, M.A.; Tartarini, P. Spray cooling by gently-deposited droplets: Experiments and modeling of heat-transfer mechanisms. In Proceedings of the 15th International Heat Transfer Conference (IHTC-15), Kyoto, Japan, 10–15 August 2014.

123. Fly, A.; Thring, R.H. A comparison of evaporative and liquid cooling methods for fuel cell vehicles. *Int. J. Hydrogen Energy* **2016**, *41*, 14217–14229. [CrossRef]

124. Santangelo, P.E.; Corticelli, M.A.; Tartarini, P. Experimental and numerical analysis of thermal interaction between two droplets in spray cooling of heated surfaces. *Heat Transf. Eng.* **2018**, *39*, 217–228. [CrossRef]

125. Ramezanizadeh, M.; Alhuyi Nazar, M.; Hossein Ahmadi, M.; Chen, L. A review on the approaches applied for cooling fuel cells. *Int. J. Heat Mass Transf.* **2019**, *139*, 517–525. [CrossRef]

126. Berg, P.; Promislow, K.; St Pierre, J.; Stumper, J.; Wetton, B. Water management in PEM Fuel Cells. *J. Electrochem. Soc.* **2004**, *151*, A341. [CrossRef]

127. Hassan, N.S.M.; Daud, W.R.W.; Sopian, K.; Sahari, J. Water management in a single cell proton exchange membrane fuel cells with a serpentine flow field. *J. Power Sources* **2009**, *193*, 249–257. [CrossRef]

128. Andersson, M.; Beale, S.B.; Espinoza, M.; Wu, Z.; Lehnert, W. A review of cell-scale multiphase flow modeling, including water management, in polymer electrolyte fuel cells. *Appl. Energy* **2016**, *180*, 757–778. [CrossRef]

129. Santangelo, P.E.; Tartarini, P. Effects of load variation and purge cycles on the efficiency of Polymer Electrolyte Membrane Fuel Cells for stationary applications. *J. Renew. Sustain. Energy* **2018**, *10*, 014301. [CrossRef]

130. Gutru, R.; Turtayeva, Z.; Xu, F.; Maranzana, G.; Vigolo, B.; Desforges, A. A comprehensive review on water management strategies and developments in anion exchange membrane fuel cells. *Int. J. Hydrogen Energy* **2020**, *45*, 19642–19663. [CrossRef]

131. Wang, X.R.; Ma, Y.; Gao, J.; Li, T.; Jiang, G.Z.; Sun, Z.Y. Review on water management methods for proton exchange membrane fuel cells. *Int. J. Hydrogen Energy* **2021**, *46*, 12206–12229. [CrossRef]
132. Zhang, B.; Hua, Y.; Gao, Z. Strategies to optimize water management in anion exchange membrane fuel cells. *J. Power Sources* **2022**, *525*, 231141. [CrossRef]